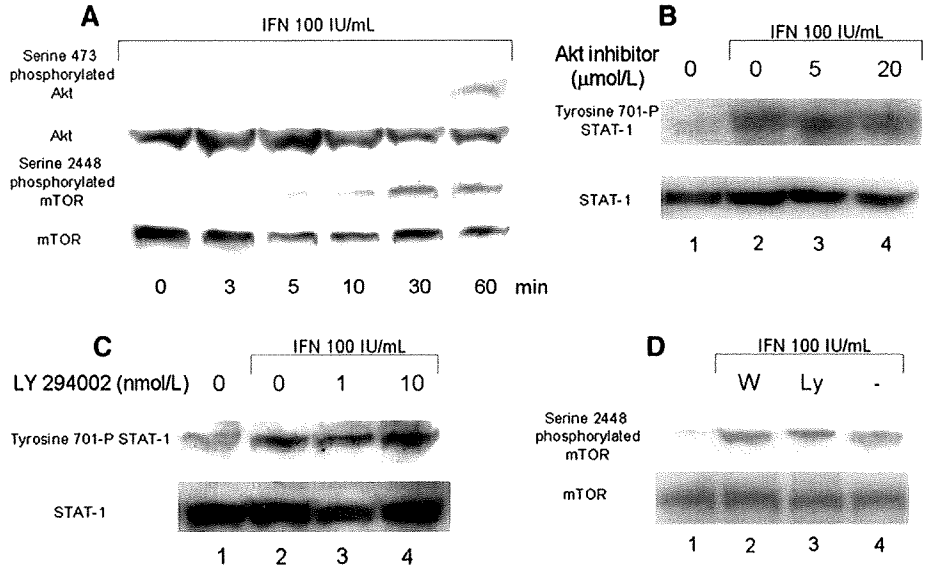

Fig. 2 Effect of IFN-α on Akt and mTOR (**a**) and effect of Akt inhibitor (**b**) and LY294002 (**c**) on IFN-α-induced tyrosine phosphorylated STAT-1 and Serine phosphorylated mTOR (**d**). Hc cells were stimulated by 100 IU/L IFN-α for 60 min. At the indicated time, the cells were harvested. Phosphorylated Akt at serine-473 residue (*first panel*), Akt (*second panel*), mTOR at serine-2448 residue (*third panel*) and mTOR (*fourth panel*) were analyzed by Western blotting. After pretreatment with 5 or 20 μmol/L Akt inhibitor (*lane 3*, and 4, respectively) (**b**) and 1 or 10 nmol/L LY294002 (*lane 3* and *4*, respectively) (**c**) for 3 h, Hc cells were untreated (*lane 1*) or treated with 100 IU/mL IFN-α (*lanes 2–4*) for 5 min and phosphorylated STAT-1 at tyrosine-701 residue (*first panel*), expression of STAT-1 (*second panel*) were analyzed by Western blotting. **d** After pretreatment with 100 nmol/L wortmannin (*lane 2*) and 1 nmol/L LY294002 (*lane 3*) for 3 h, the Hc cells were either untreated (*lane 1*) or treated with 100 IU/mL IFN-α (*lanes 2–4*) for 10 min and then were phosphorylated mTOR at Serine-2448 residue (*first panel*), the expression of mTOR (*second panel*) was analyzed by Western blotting

Akt by 100 IU/ml of IFN-α was detected at 5 min and at 60 min after IFN-α treatment, respectively (Fig. 2a). The band intensity of serine 2448 phosphorylated mTOR increased at 30 min and decreased at 60 min after IFN-α treatment. In contrast, a slight band intensity of serine phosphorylated 473 Akt was only detected at 60 min after IFN-α treatment. In addition, a Western blot analysis of phosphorylated serine 2481 of mTOR and threonine 308 Akt was conducted under the same conditions as Fig. 2a, but no bands were detected (data not shown). In Fig. 2d, IFN-α-induced Serine 2448 phosphorylated mTOR was not inhibited by PI3-K inhibitors (lanes 2, 3).

The IFN-α-induced nuclear translocation of tyrosine phosphorylated STAT-1 was inhibited by pretreatment with rapa

The location of tyrosine phosphorylated STAT-1 was evaluated by fluorescence immunohistochemistry of cultured Hc cells (Fig. 3). The IFN-α-induced nuclear translocation of tyrosine phosphorylated STAT-1 was observed (Fig. 3c), but its translocation was inhibited by pretreatment with rapa and the inhibition of the translocation of STAT-1 was more definitive at 1000 nmol/L rapa (Fig. 3e) than 100 nmol/L (Fig. 3g).

IFN-α-induced ISRE-contained promoter activity is inhibited by pretreatment of rapa, but not by wortmannin, LY294002 and Akt inhibitor

The influence of pretreatment of PI3-K-Akt-mTOR inhibitors on IFN-α inducible luciferase activity of the ISRE-containing promoter was examined. Since Hc cells were not sufficient for reporter gene transfection, HuH-7 cells were used in the transfection assay. HuH-7 cells were transfected with pISRE-Luc containing five repeats of the ISRE sequence and pRV-SV40 as a standard and then were treated with IFN-α after 3 h with or without pretreatment with rapa, wortmannin, LY294002 or Akt inhibitor. Rapa inhibited IFN-α inducible luciferase activity in a dose-dependent manner (Fig. 4, lane 2–4). However, wortmannin and LY294002, PI3-K inhibitor, and Akt inhibitor had no effect on IFN-α inducible luciferase activity (Fig. 4, lanes 2, 5–7).

The expression of IFN-α-induced tyrosine phosphorylated STAT-1 was determined after pretreatment with Akt inhibitor and LY294002 to evaluate the result of luciferase assay (Fig. 4). The Hc cells were incubated under the same conditions used in Fig. 4, but phosphorylated STAT-1 was not inhibited by the Akt inhibitor (Fig. 2b) and LY294002 (Fig. 2c).

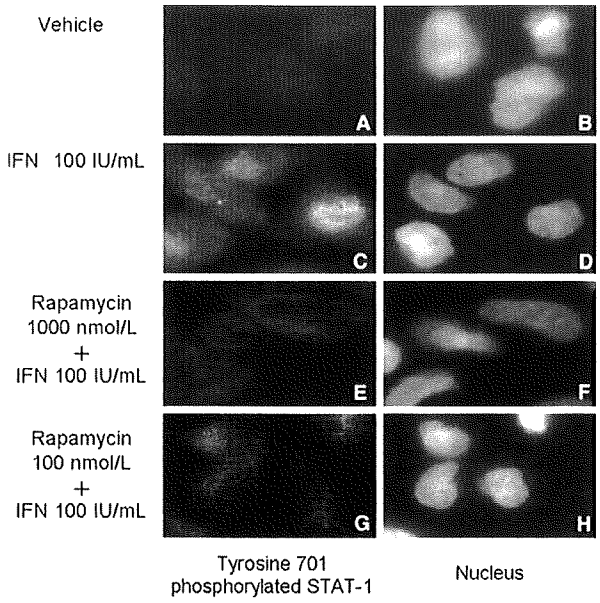

Fig. 3 Inhibition of IFN-α-induced nuclear translocation of phosphorylated STAT-1 by rapamycin. The Hc cells were pretreated without (**a–d**) or with 1000 nmol/L rapa (**e**, **f**) or 100 nmol/L rapa (**g**, **h**). After pretreatment, the Hc cells were stimulated by 100 IU/L IFN-α (**c–h**) for 30 min. Thereafter, the cells were fixed, permeabilized, processed for immunofluorescence (**a**, **c**, **e**, **g**) and Hoechst staining (**b**, **d**, **f**, **h**), and visualized by fluorescence microscopy. The results shown are from one representative experiment from a total of three performed

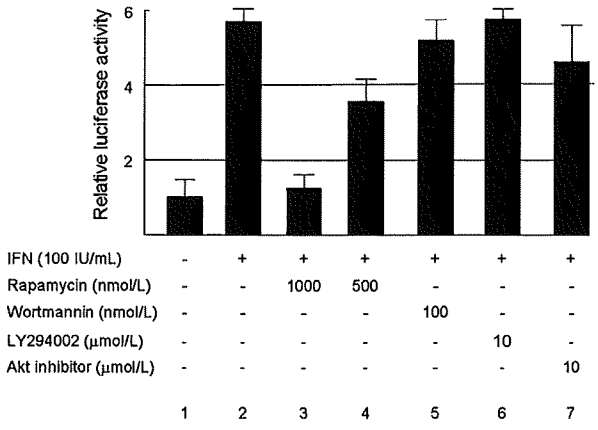

Fig. 4 Suppression effect of rapamycin, not PI3-k inhibitors and Akt inhibitor, on IFN-α-induced reporter gene assay. HuH-7 cells transfected with reporter gene (pISRE-Luc and pRL-SV40) were either untreated (*lane 1*) or pretreated with rapa (*lane 3*, *4*), wortmannin (*lane 5*), LY294002 (*lane 6*) or Akt inhibitor (*lane 7*) for 3 h, followed by IFN-α 100 IU/mL (*lanes 2–7*). Six hour later, the relative ISRE-luciferase activity ($n = 4$) was determined as described in the "Materials and methods". The data are expressed as the mean ± SD and are representative example of four similar experiments

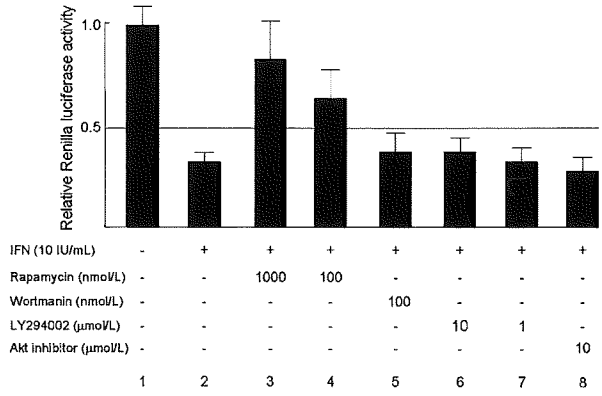

Fig. 5 Alternation of IFN-α suppressed HCV replication by rapamycin, but not PI3-K inhibitors and Akt inhibitor. OR6 cells, a full-length replicon system, were treated with 100 IU/mL of IFN-α in the absence (*lane 2*) or presence of pretreatment (*lanes 3–8*) for 3 h. *Lane 1* was not treated IFN-α alone. One day latter, *Renilla* luciferase activity was determined by luminometer ($n = 4$). The data are expressed as the mean ± SD and are representative example of four similar experiments

Rapamycin and mTOR specific siRNA, but not PI3-K inhibitor and Akt inhibitor can cancel the IFN-α-induced anti-HCV replicon activity

OR6 cells the full-length HCV replication system was used to examine the anti-viral effect of PI3-K, Akt and mTOR on IFN-α stimulation. The cells were treated with IFN-α after 3 h in the presence or absence of rapa, Akt inhibitor or PI3-K inhibitor (Fig. 5). Pretreatment with rapa attenuated its anti-HCV replication effect in comparison to IFN-α alone (Fig. 5, lanes 1–4), whereas pretreatment with PI3-K inhibitors and Akt inhibitor did not increase the *Renilla* luciferase activity (Fig. 5, lanes 1, 2, 5–8). We performed siRNA transfection for mTOR knock down (Fig. 6). Although transfection efficiency of siRNA is barely 10%, IFN-α-induced anti-HCV action was clearly inhibited in siRNA against mTOR transfected cells (lane 5) in comparison to the control cells (lane 6).

Discussion

Rapa inhibited the IFN-α-induced tyrosine and serine phosphorylation and nuclear translocation of STAT-1, the ISRE-promoter activity, the expression of PKR and the replication of HCV replicon. This suggests that the IFN-induced mTOR activity, through Jak independent STAT-1 phosphorylation, is a critical signal for IFN-induced anti-HCV action. Interestingly, mTOR activated by IFN was PI3-K-Akt independent in this study.

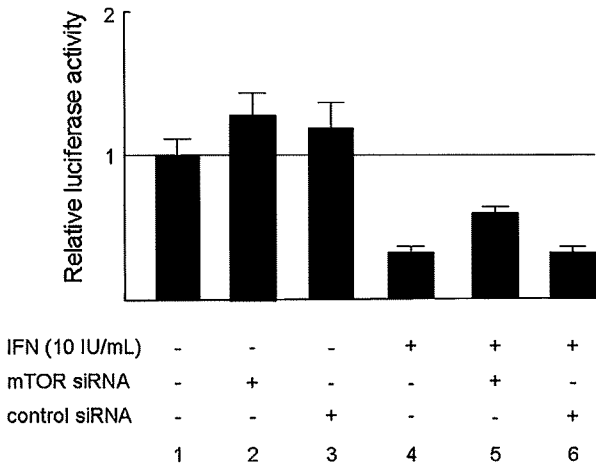

Fig. 6 Alternation of IFN-α suppressed HCV replication by siRNA against mTOR. The OR6 cells were transfected the siRNA against mTOR (*lanes 2, 5*) and the non-targeted siRNA (*lanes 3, 6*). One day later, the cells were IFN-α treatment (*lanes 4–6*). HCV replicon assay is same as Fig. 5. The data are expressed as the mean ± SD and are representative example of four similar experiments

mTOR activity may have an inhibitory action on HCV replication through STAT-1 phosphorylation, but not the translation initiation action of mTOR. This study assumed that IFN-induced PKR expression and ISRE-luciferase activity were inhibited by rapa as the result of a suppression effect on IFN inducible STAT-1 activation. IFN inducible PKR contributes the anti-HCV action [20], and anti-HCV action of ribavirin is also attributable to its ability to up-regulate PKR activity [21]. Previous reports revealed that the mTOR activity did not influence the HCV-IRES activity because the viral promoter has cap-independent translation [23]. Although mTOR is the mRNA translational regulator through phosphorylation of a downstream target such as 4E-BP and S6K [24], we think that the IFN-induced mTOR activity influences the phosphorylation of STAT-1 in our study (Fig. 1). In addition, it is thought that the alternation of STAT-1 phosphorylation by the mTOR activity influences the gene expression of anti-virus protein and IFN-induced anti-viral action.

In our study, serine-473 on Akt showed a delayed phosphorylation in comparison to that of serine-2448 on mTOR after IFN stimulation (Fig. 2a). Since serine-473 on Akt is phosphorylated by mTOR/Rictor/GβL [25, 26] and a PDK-1 independent pathway [25], IFN-induced serine-473 phosphorylated Akt may not involve the mTOR activity. Therefore, PI3-K inhibitor and Akt inhibitor had no effect on IFN inducible anti-HCV action. The pathway of mTOR activation is prismatic. PI-3Ks, upstream kinase of Akt and mTOR, are grouped into three classes (I–III), according to their substrate preference and sequence homology [27]. PI3-k inhibitor, wortmannin and LY294002, inhibit class I and III PI3-Ks, and to a lesser extent class II PI3-K, upstream kinase of Akt [27]. In our study, neither PI3-K nor Akt inhibitor inhibited IFN-induced ISRE luciferase activity and loss of HCV replication (Figs. 4, 5). These results indicate that the IFN-induced anti-HCV activity is mTOR dependent, but not PI3-K and Akt dependent. In the current report, the production of IL-1 receptor antagonist in IFN-stimulated monocytes depends on the PI3-K pathway, but not STAT-1 [28], and chronic myelogenous leukemia cells are differentially regulated by the IFN-induced PI3-K-Akt-mTOR pathway with no relation to STAT-1 phosphorylation [29]. Similar to the findings of those reports, the PI3-K-Akt pathway has been reported to be generally independent of the STAT activity [10]. Therefore, the difference in the cell type [8] may explain the discrepancy between these data and our data. We therefore speculate that in hepatocytes, unlike lymphoid cells, IFN-induced mTOR activity is not dependent on the PI3-K activity. In addition, the mTOR activity is not related to the STAT activity in lymphoid cells. However, in hepatocytes, the IFN-induced mTOR activity was closely linked to the IFN-induced STAT activity in our study.

mTOR is a serine and threonine kinase [10]. Phosphorylation of STATs by mTOR occurs also on a serine residue, but not tyrosine [10, 30]. The mTOR pathway is critical for IFN-γ-induced suppression of tyrosine phosphorylated STAT-3 in a prostate cancer cell line [31]. Although this is not consistent with the results of our study, this also showed mTOR to be associated with tyrosine phosphorylation without reference to SOCS and phosphatase. In addition, in a mouse embryo fibroblast cell line, IFN-γ-induced tyrosine and serine phosphorylation of STAT-1 is inhibited by rapa [32], while in the hepatoma cell line, HLF, IFN-β stimulated STAT-1 tyrosine phosphorylation partially decreases by LY294002, but the effect of rapa has not yet been studied [33]. In the current study [31–33], not only STAT-1 serine phosphorylation but also tyrosine was found to be downstream of the IFN induced mTOR activity; however, the mechanism controlling the tyrosine phosphorylation of STAT-1 and the mTOR activity, remains to be elucidated.

In conclusion, IFN-induced mTOR activity, independent of PI3-K and Akt, is the critical factor for anti-HCV action. The Jak independent mTOR activity is, therefore, involved in STAT-1 phosphorylation and nuclear location, thus resulting in the development of IFN-induced anti-HCV protein, especially the expression of PKR, in HCV-infected hepatocytes.

References

1. Fattovich G, Stroffolini T, Zagni I, Donato F. Hepatocellular carcinoma in cirrhosis: incidence and risk factors. Gastroenterology. 2004;127:S35–50.
2. Pawlotsky JM, Chevaliez S, McHutchison JG. The hepatitis C virus life cycle as a target for new antiviral therapies. Gastroenterology. 2007;132:1979–98.
3. Persico M, Capasso M, Persico E, Svelto M, Russo R, Spano D, et al. Suppressor of cytokine signaling 3 (SOCS3) expression and hepatitis C virus-related chronic hepatitis: insulin resistance and response to antiviral therapy. Hepatology. 2007;46:1009–15.
4. Walsh MJ, Jonsson JR, Richardson MM, Lipka GM, Purdie DM, Clouston AD, et al. Non-response to antiviral therapy is associated with obesity and increased hepatic expression of suppressor of cytokine signaling 3 (SOCS-3) in patients with chronic hepatitis C, viral genotype 1. Gut. 2006;55:529–35.
5. Huang Y, Feld JJ, Sapp RK, Nanda S, Lin JH, Blatt LM, et al. Defective hepatic response to interferon and activation of suppressor of cytokine signaling 3 in chronic hepatitis C. Gastroenterology. 2007;132:733–44.
6. Taylor MW, Tsukahara T, Brodsky L, Schaley J, Sanda C, Stephens MJ, et al. Changes in gene expression during pegylated interferon and ribavirin therapy of chronic hepatitis C virus distinguish responders from nonresponders to antiviral therapy. J Virol. 2007;81:3391–401.
7. Lan KH, Lan KL, Lee WP, Sheu ML, Chen MY, Lee YL, et al. HCV NS5A inhibits interferon-alpha signaling through suppression of STAT1 phosphorylation in hepatocyte-derived cell lines. J Hepatol. 2007;46:759–67.
8. van Boxel-Dezaire AH, Rani MR, Stark GR. Complex modulation of cell type-specific signaling in response to type I interferons. Immunity. 2006;25:361–72.
9. Ichikawa T, Nakao K, Nakata K, Yamashita M, Hamasaki K, Shigeno M, et al. Involvement of IL-1beta and IL-10 in IFN-alpha-mediated antiviral gene induction in human hepatoma cells. Biochem Biophys Res Commun. 2002;294:414–22.
10. Kaur S, Uddin S, Platanias LC. The PI3' kinase pathway in interferon signaling. J Interferon Cytokine Res. 2005;25:780–7.
11. Kaur S, Lal L, Sassano A, Majchrzak-Kita B, Srikanth M, Baker DP, et al. Regulatory effects of mammalian target of rapamycin-activated pathways in type I and II interferon signaling. J Biol Chem. 2007;282:1757–68.
12. Kudchodkar SB, Del Prete GQ, Maguire TG, Alwine JC. AMPK-mediated inhibition of mTOR kinase is circumvented during immediate-early times of human cytomegalovirus infection. J Virol. 2007;81:3649–51.
13. Minami K, Tambe Y, Watanabe R, Isono T, Haneda M, Isobe K, et al. Suppression of viral replication by stress-inducible GADD34 protein via the mammalian serine/threonine protein kinase mTOR pathway. J Virol. 2007;81:11106–15.
14. Ishida H, Li K, Yi M, Lemon SM. p21-activated kinase 1 is activated through the mammalian target of rapamycin/p70 S6 kinase pathway and regulates the replication of hepatitis C virus in human hepatoma cells. J Biol Chem. 2007;282:11836–48.
15. Guo H, Zhou T, Jiang D, Cuconati A, Xiao GH, Block TM, et al. Regulation of hepatitis B virus replication by the phosphatidylinositol 3-kinase-Akt signal transduction pathway. J Virol. 2007;81:10072–80.
16. Mannova P, Beretta L. Activation of the N-Ras-PI3K-Akt-mTOR pathway by hepatitis C virus: control of cell survival and viral replication. J Virol. 2005;79:8742–9.
17. Nishimura D, Ishikawa H, Matsumoto K, Shibata H, Motoyoshi Y, Fukuta M, et al. DHMEQ, a novel NF-kappaB inhibitor, induces apoptosis and cell-cycle arrest in human hepatoma cells. Int J Oncol. 2006;29:713–9.
18. Ikeda M, Abe K, Dansako H, Nakamura T, Naka K, Kato N. Efficient replication of a full-length hepatitis C virus genome, strain O, in cell culture, and development of a luciferase reporter system. Biochem Biophys Res Commun. 2005;329:1350–9.
19. Obora A, Shiratori Y, Okuno M, Adachi S, Takano Y, Matsushima-Nishiwaki R, et al. Synergistic induction of apoptosis by acyclic retinoid and interferon-beta in human hepatocellular carcinoma cells. Hepatology. 2002;36:1115–24.
20. Wang C, Pflugheber J, Sumpter R Jr, Sodora DL, Hui D, Sen GC, et al. Alpha interferon induces distinct translational control programs to suppress hepatitis C virus RNA replication. J Virol. 2003;77:3898–912.
21. Liu WL, Su WC, Cheng CW, Hwang LH, Wang CC, Chen HL, et al. Ribavirin up-regulates the activity of double-stranded RNA-activated protein kinase and enhances the action of interferon-alpha against hepatitis C virus. J Infect Dis. 2007;196:425–34.
22. Tamada Y, Nakao K, Nagayama Y, Nakata K, Ichikawa T, Kawamata Y, et al. p48 Overexpression enhances interferon-mediated expression and activity of double-stranded RNA-dependent protein kinase in human hepatoma cells. J Hepatol. 2002;37:493–9.
23. Dowling RJ, Zakikhani M, Fantus IG, Pollak M, Sonenberg N. Metformin inhibits mammalian target of rapamycin-dependent translation initiation in breast cancer cells. Cancer Res. 2007;67:10804–12.
24. Mamane Y, Petroulakis E, LeBacquer O, Sonenberg N. mTOR, translation initiation and cancer. Oncogene. 2006;25:6416–22.
25. Hanada M, Feng J, Hemmings BA. Structure, regulation and function of PKB/AKT–a major therapeutic target. Biochim Biophys Acta. 2004;1697:3–16.
26. Hresko RC, Mueckler M. mTOR.RICTOR is the Ser473 kinase for Akt/protein kinase B in 3T3–L1 adipocytes. J Biol Chem. 2005;280:40406–16.
27. Engelman JA, Luo J, Cantley LC. The evolution of phosphatidylinositol 3-kinases as regulators of growth and metabolism. Nat Rev Genet. 2006;7:606–19.
28. Molnarfi N, Hyka-Nouspikel N, Gruaz L, Dayer JM, Burger D. The production of IL-1 receptor antagonist in IFN-beta-stimulated human monocytes depends on the activation of phosphatidylinositol 3-kinase but not of STAT1. J Immunol. 2005;174:2974–80.
29. Parmar S, Smith J, Sassano A, Uddin S, Katsoulidis E, Majchrzak B, et al. Differential regulation of the p70 S6 kinase pathway by interferon alpha (IFNalpha) and imatinib mesylate (STI571) in chronic myelogenous leukemia cells. Blood. 2005;106:2436–43.
30. Nguyen H, Ramana CV, Bayes J, Stark GR. Roles of phosphatidylinositol 3-kinase in interferon-gamma-dependent phosphorylation of STAT1 on serine 727 and activation of gene expression. J Biol Chem. 2001;276:33361–8.
31. Fang P, Hwa V, Rosenfeld RG. Interferon-gamma-induced dephosphorylation of STAT3 and apoptosis are dependent on the mTOR pathway. Exp Cell Res. 2006;312:1229–39.
32. El-Hashemite N, Zhang H, Walker V, Hoffmeister KM, Kwiatkowski DJ. Perturbed IFN-gamma-Jak-signal transducers and activators of transcription signaling in tuberous sclerosis mouse models: synergistic effects of rapamycin-IFN-gamma treatment. Cancer Res. 2004;64:3436–43.
33. Matsumoto K, Okano J, Murawaki Y. Differential effects of interferon alpha-2b and beta on the signaling pathways in human liver cancer cells. J Gastroenterol. 2005;40:722–32.

Liver International ISSN 1478-3223

CLINICAL STUDIES

Differences in molecular alterations of hepatocellular carcinoma between patients with a sustained virological response and those with hepatitis C virus infection

Takehiro Hayashi[1,2], Akihiro Tamori[1], Manabu Nishikawa[3], Hiroyasu Morikawa[1], Masaru Enomoto[1], Hiroki Sakaguchi[1], Daiki Habu[1], Norifumi Kawada[1], Shoji Kubo[4], Shuhei Nishiguchi[5] and Susumu Shiomi[2]

1 Department of Hepatology, Osaka City University Graduate School of Medicine, Osaka, Japan
2 Department of Nuclear Medicine, Osaka City University Graduate School of Medicine, Osaka, Japan
3 Department of Biochemistry and Molecular Pathology, Osaka City University Graduate School of Medicine, Osaka, Japan
4 Department of Surgery, Osaka City University Graduate School of Medicine, Osaka, Japan
5 Department of Internal Medicine, Hyogo College of Medicine, Nishinomiya, Japan

Keywords
hepatitis C virus – hepatocellular carcinoma – hypermethylation – interferon – mitochondrial DNA – *p16* – *p53* – sustained virological response

Correspondence
Akihiro Tamori, MD, Department of Hepatology, Osaka City University Graduate School of Medicine, 1-4-3 Asahimachi, Abeno-ku, Osaka 545-8585, Japan
Tel: +81 6 6645 2292
Fax: +81 6 6645 1433
e-mail: atamori@med.osaka-cu.ac.jp

Received 16 January 2008
Accepted 16 March 2008

DOI:10.1111/j.1478-3231.2008.01772.x

Abstract
Background/Aims: The mechanism of hepatocarcinogenesis remains unclear in patients in whom hepatitis C virus (HCV) disappears after interferon (IFN) therapy. We compared molecular alterations in hepatocellular carcinoma (HCC) between patients with a sustained virological response (SVR) to IFN and patients with HCV. *Methods:* The study group comprised 44 patients with HCV and 13 patients with SVR. One patient in the SVR group had two tumour nodules, both of which were examined. Mitochondrial DNA (mtDNA) mutations in displacement-loop lesions were directly sequenced. Mutation of the TP53 gene was examined by direct sequencing. The methylation status of *p16*, *p15*, *p14*, *RB* and *PTEN* genes was evaluated by a methylation-specific polymerase chain reaction. *Results:* The average number of mtDNA mutations was 4.2 in 44 HCCs with HCV and 2.0 in 14 HCCs with SVR ($P = 0.0021$). mtDNA mutation was less frequently detected in HCCs from patients with SVR than in patients with HCV. TP53 mutations were detected in 12 (27%) of 44 HCCs with HCV and 2 (14%) of 14 SVR-HCCs. Hypermethylation of the *p16*, *p15*, *p14*, *RB* and *PTEN* promoters was, respectively, detected in 34, 13, 8, 12 and 11 of 44 HCCs from patients with HCV and 14, 0, 0, 2 and 2 of 14 HCCs from patients with SVR ($P = 0.049$, 0.021, 0.085, 0.322 and 0.402). Hypermethylation of *p16* was one of the most important alterations in SVR-HCC. *Conclusions:* Molecular alterations in hepatocarcinogenesis of patients with SVR-HCC were different from those of patients with continuous HCV infection.

Hepatitis C virus (HCV) is one of the most important risk factors for hepatocellular carcinoma (HCC). Clinical studies have suggested that HCV induces inflammation in the liver, followed by the accumulation of reactive oxygen species (ROS), which promote mutations in the human genome (1, 2). Persistent inflammation also results in repeated hepatocyte death and regeneration, leading to the gradual accumulation of DNA mutations in hepatocytes. Point mutations in tumour suppressor genes, including TP53, have been confirmed in hepatic cirrhosis in patients with HCV (3). Epigenetic alterations, such as methylation of the promoter of cell cycle gene inhibitors with the resulting loss of its expression, have been frequently detected in liver cirrhosis with viral infection (4, 5). Continuous inflammation induces genetic or epigenetic alterations, or both, in hepatocytes, culminating in a preneoplastic condition. HCV itself is an oncogenic virus. HCV core protein or HCV NS5A protein has oncogenic potential function in animal models without inflammation (6, 7). *In vitro* studies have suggested that HCV protein modifies host immunity to sustain infection (8). The suppression of immunological response is attributed to the failure to eliminate neoplastic cells from the liver. These findings suggest that cooperation between virus-induced chronic inflammation and HCV coding proteins accelerates carcinogenesis in the liver.

Interferon (IFN) has potent antiviral activity against HCV. Antiviral therapy with pegylated IFN in combination with ribavirin produces a sustained virological response (SVR) in approximately 60% of patients with chronic hepatitis C (9, 10). Complete eradication of HCV by antiviral therapy is associated with a considerable reduction in the incidence of HCC (11, 12). Nevertheless, recent studies have shown that HCC develops in 2.5–4.2% of patients after eradication of HCV by IFN therapy (13–15). It is therefore important to delineate important features of HCC that develop after the elimination of HCV as compared with those established during sustained HCV infection. Makiyama *et al.* (15) speculated that cancer cells already exist in the liver before HCV eradication by IFN treatment. The integration of HBV DNA because of past HBV infections (16) or occult HCV infections (17) may be linked to SVR-HCC. However, the molecular mechanism leading to the development of SVR-HCC remains obscure.

In the present study, we compared genetic alterations in surgically resected specimens of HCCs between patients with SVR and those with continuous HCV infection. Our results might contribute to a better understanding of the molecular changes in

the liver of patients in whom HCC develops after the eradication of HCV.

Patients and methods

Patients

Thirteen consecutive patients who underwent surgical resection of HCC in Osaka City University Hospital after eradication of HCV by IFN monotherapy from 1998 June through 2007 July (SVR group) were studied (Table 1). One patient in the SVR group had two tumour nodules, both of which were examined. As a control, 44 HCV-RNA-positive patients with HCC were studied. Thus, 58 HCC samples and 57 noncancerous tissue samples were evaluated. One portion of each sample was frozen in liquid nitrogen immediately after resection and stored at − 80 °C until analysis. Total RNA and DNA were extracted from these portions by conventional methods as described previously (18). None of the patients had a history of exposure to aflatoxin B1, more than 30 g/day of alcohol intake, insulin administration, hereditary haemochromatosis or other liver diseases such as hepatitis B, autoimmune hepatitis and primary biliary cirrhosis. The activity of hepatitis and stage of fibrosis were determined according to a modified version of Desmet's classification in liver tissue specimens before IFN therapy and in noncancerous liver tissue obtained intra-operatively (19).

Table 1. Clinical characteristics of patients with sustained virological response-hepatocellular carcinoma and hepatitis C virus-hepatocellular carcinoma

	SVR-HCC	HCV-HCC	*P*-value
n	13	44	
Male/female	13/0	44/0	
Age	64.3 (55–73)	64.0 (34–79)	0.977
Anti-HCV(+)/ HCV-RNA(+)	13/0	44/44	
HBs antigen positivity	0	0	
IFN therapy	13	0	
ALT (IU/L)	35.0 (17–81)	73.2 (13–188)	0.0001
Diabetes mellitus			
With/without/ unknown	2/11/0	13/28/3	0.25
Alcohol habits			
Positive/negative/ unknown	5/8/0	23/17/4	0.23
Tumour differentiation			
Well/moderately/ poorly	0/4/10	5/20/19	0.066
Noncancerous liver			
Cirrhosis/noncirrhosis	4/9	20/24	0.34
Tumour diameter (mm) (average)	43.1 (12–125)	38.3 (10–180)	0.756
Extrahepatic metastasis	0	0	

ALT, alanine aminotransferase; HBs antigen, hepatitis B surface antigen; HCC, hepatocellular carcinoma; HCV, hepatitis C virus; IFN, interferon; SVR, sustained virological reaction.

Sequencing the displacement-loop region of mitochondrial DNA

Each DNA sample (50 ng) was subjected to amplification by polymerase chain reaction (PCR) with the use of overlapping sets of primers to screen the entire mitochondrial genome. To avoid coamplification of nuclear pseudogenes, the primers were selected with the use of mitochondrial DNA (mtDNA)-depleted cells established as described previously (2, 20). PCR (an initial incubation at 94 °C for 5 min, followed by 35 cycles of 94 °C for 30 s, 55 °C for 30 s and 72 °C for 1 min) was performed in a final volume of 50 µl with a GeneAmp PCR system 9600 (Perkin-Elmer Life Sciences Japan, Tokyo, Japan). Aberrant PCR products were purified with a QIAquick PCR purification kit (Qiagen, Tokyo, Japan) and sequenced with an Applied Biosystems DNA sequencer (Perkin-Elmer Life Sciences Japan) and a Dye Terminator Cycle Sequencing FS Ready Reaction kit (*Applied* Biosystems, Tokyo, Japan). The sequence of the displacement (D)-loop (nucleotides 100–600) was examined for all 57 patients with HCC. All mutations were confirmed by repeated DNA sequencing.

Direct sequencing for TP53

We directly sequenced exons 5 through 8 of TP53 genes, in which 98% of TP53 mutations are detected (21), in 58 tumours. One hundred nanograms of genomic DNA was subjected to 35 PCR cycles (94, 55 and 72 °C for 0.5, 0.5 and 1 min respectively) with rTaq DNA polymerase (TakaraBio Co. Ltd, Otsu, Japan). After the PCR products were purified with a QIAquick PCR purification kit, we sequenced the amplified products with a DNA sequencing system and a Dye Terminator Cycle Sequencing FS Ready Reaction kit.

Methylation-specific polymerase chain reaction

Bisulphite modification of genomic DNA was performed as described by Herman *et al.* (22). Briefly, 1 µg of DNA was denatured with NaOH, and 10 mM hydroquinone and 3 M sodium bisulphite were successively added to the mixture. The sample was incubated at 50 °C for 16 h. Modified DNA was purified with the use of Wizard DNA purification resin (Promega Corporation, Madison, WI, USA), followed by ethanol precipitation. DNA methylation patterns were determined by chemical modification of the unmethylated cytosines to uracil and subsequent PCR, using primers specific for either methylated or modified unmethylated DNA. The primers used in this study are shown in Table 2 (23, 24). The PCR amplification procedure has been described previously (5). Ten microlitres of each PCR product was loaded directly onto nondenaturing 2% agarose gels, stained with ethidium bromide and visualized under ultraviolet illumination.

Semiquantitative reverse-transcription polymerase chain reaction analysis

To investigate *p16* mRNA expression, we performed reverse-transcription PCR (RT-PCR) with total RNA from 35 tumours and 27 noncancerous lesions. Briefly, 1 µg of the RNA was used as a template to generate complementary DNA (cDNA) using random hexamers and reverse transcriptase. The cDNA was used for PCR amplification. Primer sequences were 5′-CCACCCCGC TTTCGTAGTTTT-3′ (upper primer) and 5′-TGCGAGGCTCG CAAGAAAT-3′ (lower primer) for *p16* and 5′-CCTCGCCTT TGCCGATCC-3′ (upper primer) and 5′-GGATCTTCATGAGG TAGTCAGTC-3′ (lower primer) for β-actin. The PCR procedure for *p16* consisted of one cycle at 95 °C for 12 min, 30 cycles at 95 °C for 30 s, 51 °C for 1 min and 72 °C for 30 s, and one cycle at

Table 2. Primers used for methylation-specific polymerase chain reaction

Gene		Sequence
p16	Unmethylated	5′-TTATTAGAGGGTGGGGTGGATTGT-3′ (sense)
		5′-CAACCCCAAACCACAACCATAA-3′ (antisense)
	Methylated	5′-TTATTAGAGGGTGGGGCGGATCGC-3′ (sense)
		5′-GACCCCGAACCGCGACCGTAA-3′ (antisense)
p15	Unmethylated	5′-TGTGATGTGTTTGTATTTTGTGGTT-3′ (sense)
		5′-CCATACAATAACCAAACAACCAA-3′ (antisense)
	Methylated	5′-GCGTTCGTATTTTGCGGTT-3′ (sense)
		5′-CGTACAATAACCGAACGACCGA-3′ (antisense)
p14	Unmethylated	5′-TTTTTGGTGTTAAAGGGTGGTGTAGT-3′ (sense)
		5′-CACAAAAACCCTCACTCACAACAA-3′ (antisense)
	Methylated	5′-GTGTTAAAGGGCGGCGTAGC-3′ (sense)
		5′-AAAACCCTCACTCGCGACGA-3′ (antisense)
RB		5′-CTTTGTATAGCCCCGTTAAGTG-3′ (sense)
		5′-GTCATGAGGAATTAAACTGGGA-3′ (antisense)
PTEN	Unmethylated	5′-GTGTTGGTGGAGGTAGTTGTTT-3′ (sense)
		5′-ACCACTTAACTCTAAACCACAACCA-3′ (antisense)
	Methylated	5′-TTCGTTCGTCGTCGTCGTATTT-3′ (sense)
		5′-GCCGCTTAACTCTAAACCGCAACCG-3′ (antisense)

72 °C for 3 min. That for β-actin consisted of one cycle at 94 °C for 3 min, 24 cycles at 95 °C for 30 s, 60 °C for 1 min and 72 °C for 30 s, and one cycle at 72 °C for 3 min. Ten microlitres of each PCR product was loaded directly onto nondenaturing 8% polyacrylamide gels, and the gels were stained with SYBR Greene (BioWhittaker Molecular Applications, Rockland, ME, USA) according to the manufacturer's protocol. The intensity of the bands was quantified by densitometry.

Statistical analysis

Age, tumour size, liver function and mtDNA mutations were compared between the two groups with the Mann–Whitney *U* test. Histological findings, diabetes mellitus, alcohol use, tumour differentiation, TP53 mutation and methylation status were compared between the two groups with the χ^2 test.

Ethical considerations

This study protocol complied with the ethical guidelines of the Declaration of Helsinki (1975) and was approved by the Ethics Committee of Osaka City University Graduate School of Medical.

Results

Histological findings in patients with sustained virological response

In patients with SVR, the period from the end of IFN treatment to hepatectomy for HCC ranged from 13 to 156 months. Histological examinations, performed in 11 of the 13 patients with SVR-HCCs, showed that the staging of hepatic fibrosis improved in five patients and the grade of hepatic activity improved in eight patients (Table 3).

Mitochondrial DNA mutations of hepatocellular carcinoma

Mutations of mtDNA were found in both HCC and noncancerous liver tissue. Previously, three mutation sites in mtDNA have been reported to be unique for the Japanese. Excluding these sites, we evaluated the average number of mtDNA mutations in D-loop lesions (Table 4). The average number of mtDNA mutations in D-loop lesions was 4.2 in 44 HCCs with HCV and 2.0 in 14 HCCs from SVR patients. The average number of mtDNA mutations in D-loop lesions was 2.8 in 44 noncancerous lesions with HCV and 1.3 in 13 noncancerous lesion from SVR patients. No specific mutation in mtDNA of SVR-HCC was found in the present study. The frequency of mtDNA mutations in HCC was significantly lower in SVR patients than in HCV patients ($P = 0.0021$). The frequency of mtDNA mutations was also lower in noncancerous livers of SVR patients ($P = 0.007$). In the present study, no regularity of mtDNA mutations was found in the D-loop region.

TP53 mutation analysis

TP53 mutations were detected in 12 (27.3%) of 44 HCCs with HCV (Table 4). In detail, TP53 was mutated in codon 123, TAT to TTC; codon 132, AAG to TTG; codon 133, ATG to TTG; codon 158, CGC to CTC; codon 189, GCC to GTC; codon 220, TAT to TGT; codon 246, ATG to GTG; codon 272, GAG to GTG; codon 275, TGT to TAT; and codon 271, CAT to CGT. Two cases were mutated by insertion in exons 5 and 8. The histological findings showed that HCCs with TP53 mutations consisted of seven moderately differentiated and five poorly differentiated HCCs. TP53 mutations were detected in two (14.3%) of 14 HCCs from the 13 patients in whom HCV was eradicated by IFN therapy. In detail, TP53 was mutated in codon 135, TGC to TGG and codon 242, TGC to TTC. The histological findings showed that HCCs with TP53 mutations in SVR patients consisted of two poorly differentiated HCCs.

Methylation pattern of hepatocellular carcinoma

In patients with HCV, hypermethylation of *p16*, *p15*, *p14*, *RB* and the *PTEN* promoter was, respectively, detected in 34 (77.3%), 13 (29.5%), 8 (18.2%), 12 (27.3%) and 11 (25.0%) of 44 HCCs and 13 (29.5%), 14 (31.8%), 4 (9.1%), 11 (25.0%) and 5 (11.4%) of 44 noncancerous liver samples (Fig. 1A). In patients with SVR, hypermethylation of *p16*, *p15*, *p14*, *RB* and the *PTEN* promoter was, respectively, detected in 14 (100%), 0 (0%), 0 (0%), 2 (14.3%) and 2 (14.3%) of 14 HCCs and 2 (15.4%), 0 (0%), 0 (0%), 2 (15.4%) and 0 (0%) of 13

Table 3. Clinical course of patients with sustained virological response-hepatocellular carcinoma

Case	Pre-IFN therapy				Span for carcinogenesis after IFN therapy (months)	At operation		
	Genotype	HCV-RNA	*F* factor	*A* factor		*F* factor	*A* factor	BMI
56	1b	1 MEq	2	2	45	2	1	23.7
101	2a	+	3	2	19	4	2	23.7
149	2a	1.1 MEq	4	3	20	4	2	23.6
196	2b	+	2	2	41	1	2	23.4
198	2a	0.4 MEq	2	2	103	1	1	21.5
200	2a	1.1 MEq	2	2	13	2	1	24.6
221	2a	0.9 MEq	2	3	80	2	2	18.1
268	Unknown	+	Unknown	Unknown	144	1	1	20.3
269	2a	0.4 MEq	2	3	156	0	0	23.6
271	1b	+	4	1	156	3	1	28.1
325	1b	300 KIU	3	2	15	2	1	25.2
327	2b	160 KIU	3	3	36	4	2	26.8
328	1b	+	Unknown	Unknown	14	4	2	27.6

BMI, body mass index; HCV, hepatitis C virus; HCC, hepatocellular carcinoma; IFN, interferon; SVR, sustained virological response.

Table 4. Comparison of mutation in the displacement-loop of mitochondrial DNA, mutation in TP53 and methylation between sustained virological response-hepatocellular carcinoma and hepatitis C virus-hepatocellular carcinoma

	SVR-HCC	HCV-HCC	*P*-value
Mean mutation number in D-loop of mtDNA	2.0	4.2	0.0021
TP53 mutation	14.3%	27.3%	0.322
Methylation			
p16	100.0%	77.3%	0.049
p15	0.0%	29.5%	0.021
p14	0.0%	18.2%	0.085
RB	14.3%	27.3%	0.322
PTEN	14.3%	25.0%	0.402

D-loop, displacement-loop; HCC, hepatocellular carcinoma; HCV, hepatitis C virus; mtDNA, mitochondrial DNA; SVR, sustained virological response.

noncancerous liver samples (Fig. 1B). Methylation of *p14*, *p15*, *RB* and *PTEN* was thus slightly but not significantly more frequent in HCV-HCC than in SVR-HCC.

Expression of *p16* mRNA in hepatocellular carcinoma

Expression of *p16* mRNA was examined in 29 patients with HCV-HCC and six with SVR-HCC. In six SVR-HCCs with *p16* promoter methylation, *p16* mRNA expression was lower than that in the noncancerous liver (Fig. 2). In 29 HCV-HCCs with *p16* methylation, *p16* mRNA expression was lower than that in HCC without *p16* methylation.

Discussion

In agreement with previous studies, all patients with SVR-HCC were males in the present study (15), suggesting that sex-related factors have a role in SVR-HCC. We, therefore, studied male patients with HCV-HCC and matched subjects with SVR-HCC. First of all, mtDNA mutations were frequent in HCC as well as in noncancerous liver tissues from patients with HCV (2, 25). Chronic viral inflammation induces ROS production, followed by mtDNA damage in the liver, which is speculated to contribute to hepatocarcinogenesis (25). In contrast to mtDNA mutations, the frequency of mtDNA mutations was low in SVR liver. Histological examination of noncancerous liver tissue showed that persistent inflammation was minimal or absent in SVR patients. Nishikawa *et al.* reported that IFN therapy reduces the frequency of mtDNA mutations in the liver of patients with chronic hepatitis C. In their study, a reduced frequency of mtDNA mutations was detected only in patients whose transaminases were normalized by IFN therapy in association with HCV elimination (26). Our study also showed that the frequency of mtDNA mutations was reduced in the liver of SVR patients. In the present study, no patient with HCV-HCC received IFN. Therefore, we could not exactly clarify which factor was more closely related to fewer mtDNA mutations in SVR-HCC, IFN or HCV eradication. However, we speculate that chronic inflammation was not related to the development of HCC in SVR patients.

Destruction of tumour suppressor gene function is thought to be a critical step in carcinogenesis. Previous studies showed that TP53 mutations were detected in 27% (21) and 38.3% (27) of HCCs with viral infection. These high rates were apparently related to the late stage of hepatocarcinogenesis. In agreement with these previous reports, TP53 was mutated in seven moderately differentiated HCC and five poorly differentiated HCC (27.7%) in the 44 patients with HCV in our study. To our knowledge, no previous study has reported TP53 mutations in SVR-HCC. We found two TP53 mutations in 14 SVR-HCC, including dedifferentiated lesions. mtDNA damage induced by chronic viral hepatitis correlates with genomic injury. It was speculated that a decrease in mtDNA mutations followed loss of TP53 mutations. Although the small number of the SVR-HCCs examined in our study precludes firm conclusions, TP53 alterations might differ between SVR-HCC and HCV-HCC.

Next, we showed epigenetic alterations in both HCV-HCC and SVR-HCC. Previous studies have reported that *p16*, *p15*,

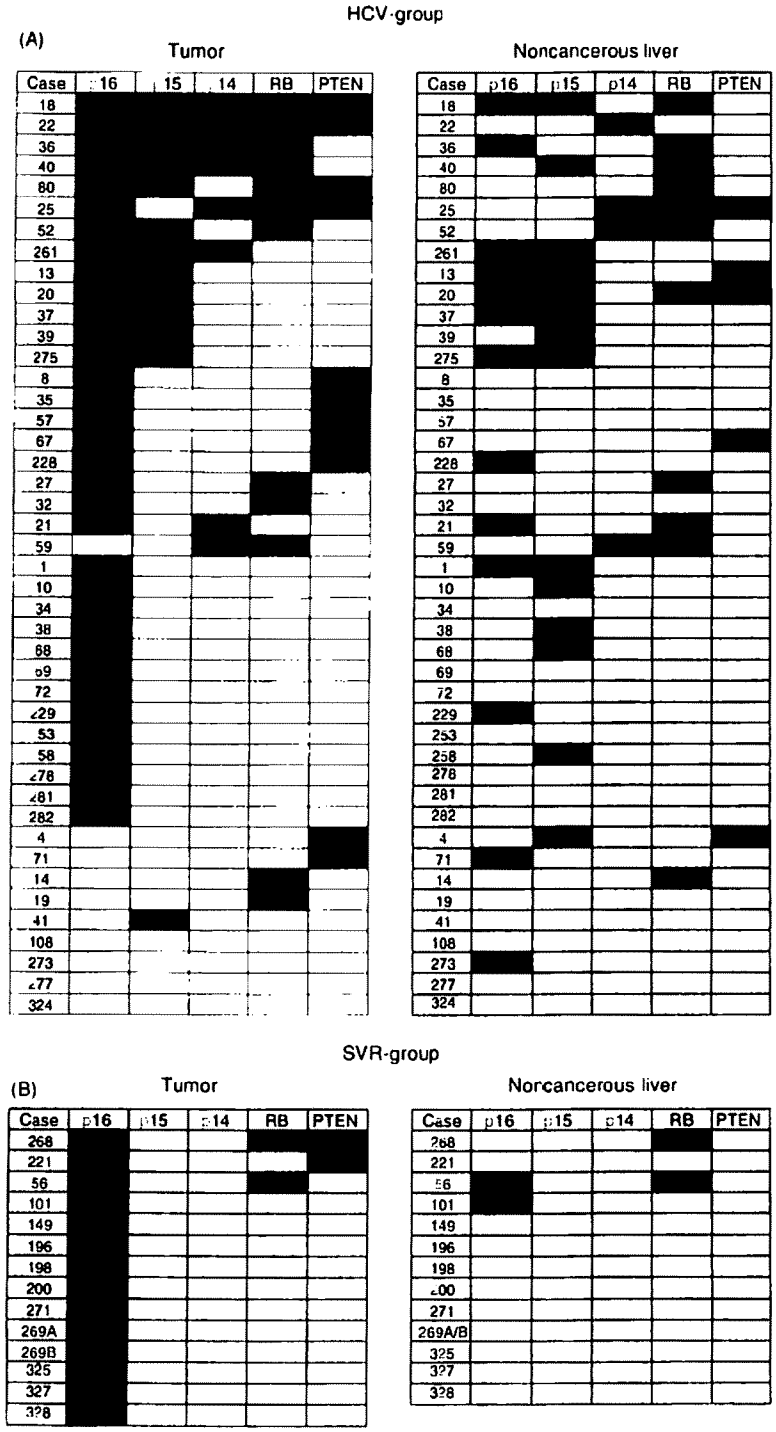

Fig. 1. Methylation patterns of *p16*, *p15*, *p14*, *RB* and *PTEN* promoter in 44 hepatocellular carcinomas (HCCs) and 44 noncancerous liver samples from the hepatitis C virus (HCV) group were examined by methylation-specific polymerase chain reaction (MSP) (A). Methylation patterns were also examined by MSP for 14 HCCs and 13 noncancerous liver samples from the sustained virological response (SVR) group (B). Black boxes indicate methylated sequences, whereas blank boxes indicate unmethylated sequences.

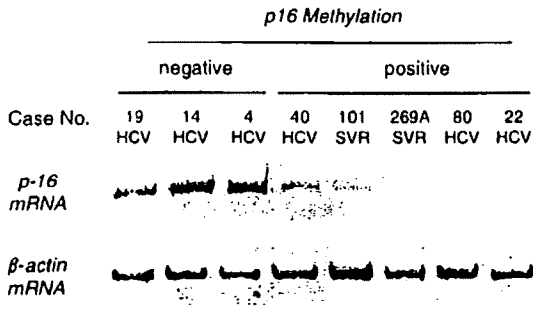

Fig. 2. Expression of *p16* mRNA in hepatocellular carcinoma (HCC). The promoter of *p16* was methylated in cases 40, 101, 269A, 80 and 22. In these tumours, *p16* expression was lower than that in HCC without methylation. β-actin expression was examined as a control. HCV, hepatitis C virus; SVR, sustained virological response.

p14, *RB* and *PTEN* are, respectively, methylated in 58–82% (4, 5, 28–32), 5–64% (5, 32–34), 0–36% (5, 32), 21% (5) and 17% (28) of HCCs from patients with viral infections. In our study, methylation of *p16*, *p15*, *p14*, *RB* and *PTEN* was, respectively, detected in 34 (77.3%), 13 (29.5%), eight (18.2%), 12 (27.3%) and 11 (25.0%) of 44 HCV-HCCs. Our findings are thus consistent with those of previous studies. In SVR-HCC, *p16* was methylated in all samples, whereas *RB* and *PTEN* were methylated in only two samples and methylation of *p15* and *p14* was not detected. This was a novel methylation profile that differed from that of SVR-HCC and HCV-HCC. We showed that promoter methylation of the *p16* gene, leading to the loss of *p16* expression, was frequently observed not only in HCV-HCC but also in SVR-HCC. These data suggested that aberrant *p16* methylation might contribute to the development of SVR-HCC.

Epidemiological studies have shown that past exposure to *Helicobacter pylori* is closely associated with an increased risk of gastric cancer and that most cases of *H. pylori*-negative gastric cancer have a history of exposure to *H. pylori* (35, 36). Maekita and colleagues reported that permanent methylation of specific CpG islands in gastric mucosae is associated with a heightened risk of gastric cancer in *H. pylori*-negative patients (37, 38). It was speculated that methylation of CpG islands in gastric stem cells led to a continuous high level of methylation in gastric mucosae (39). It was well known that HCV was spontaneously eradicated in 20% of patients with the acute infection (40). To our knowledge, there has been no report about HCC development in patients who had been cured in acute hepatitis. In the present study, *p16* was methylated in both HCC infected with HCV and HCC after eradication of HCV. We speculate that *p16* in hepatic stem cells might be methylated in the continuous presence of HCV. These cells with methylated *p16* might survive and grow after eradication of HCV by IFN therapy. Future studies should examine the methylation status of genes in successive liver specimens obtained before and after IFN therapy.

In conclusion, epigenetic alterations of some genes in SVR-HCC differed from those in HCV-HCC. Moreover, mutation of mtDNA was less common in SVR-HCC than in HCV-HCC. The present results suggest that the development of HCC in patients cured of HCV infection by IFN therapy might be associated with particular molecular alterations.

Acknowledgements

We acknowledge Ms Mayumi Shinzaki for her excellent technical assistance. This study was supported in part by a grant-in-aid from the Japan Society of the Promotion of Science (no. 16590619 to A. T.).

References

1. Marrogi AJ, Khan MA, van Gijssel HE, *et al.* Oxidative stress and p53 mutations in the carcinogenesis of iron overload-associated hepatocellular carcinoma. *J Natl Cancer Inst* 2001; 93: 1652–5.
2. Nishikawa M, Nishiguchi S, Shiomi S, *et al.* Somatic mutation of mitochondrial DNA in cancerous and noncancerous liver tissue in individuals with hepatocellular carcinoma. *Cancer Res* 2001; 61: 1843–5.
3. Minouchi K, Kaneko S, Kobayashi K. Mutation of p53 gene in regenerative nodules in cirrhotic liver. *J Hepatol* 2002; 37: 231–9.
4. Kaneto H, Sasaki S, Yamamoto H, *et al.* Detection of hypermethylation of the p16 (INK4A) gene promoter in chronic hepatitis and cirrhosis associated with hepatitis B or C virus. *Gut* 2001; 48: 372–7.
5. Roncalli M, Bianchi P, Bruni B, *et al.* Methylation framework of cell cycle gene inhibitors in cirrhosis and associated hepatocellular carcinoma. *Hepatology* 2002; 36: 427–32.
6. Moriya K, Fujie H, Shintani Y, *et al.* The core protein of hepatitis C virus induces hepatocellular carcinoma in transgenic mice. *Nat Med* 1998; 4: 1065–7.
7. Majumder M, Ghosh AK, Steele R, *et al.* Hepatitis C virus NS5A physically associates with p53 and regulates p21/waf1 gene expression in a p53-dependent manner. *J Virol* 2001; 75: 1401–7.
8. Larsson M, Babcock E, Grakoui A, *et al.* Lack of phenotypic and functional impairment in dendritic cells from chimpanzees chronically infected with hepatitis C virus. *J Virol* 2004; 78: 6151–61.
9. McHutchison JG, Gordon SC, Schiff ER, *et al.* Interferon alfa-2b alone or in combination with ribavirin as initial treatment for chronic hepatitis C. Hepatitis Interventional Therapy Group. *N Engl J Med* 1998; 339: 1485–92.
10. Manns MP, McHutchison JG, Gordon SC, *et al.* Peginterferon alfa-2b plus ribavirin compared with interferon alfa-2b plus ribavirin for initial treatment of chronic hepatitis C: a randomised trial. *Lancet* 2001; 358: 958–65.
11. Bruno S, Stroffolini T, Colombo M, *et al.* Sustained virological response to interferon-alpha is associated with improved outcome in HCV-related cirrhosis: a retrospective study. *Hepatology* 2007; 45: 579–87.
12. Yoshida H, Shiratori Y, Moriyama M, *et al.* Interferon therapy reduces the risk for hepatocellular carcinoma: national surveillance program of cirrhotic and noncirrhotic patients with chronic hepatitis C in Japan. IHIT Study Group. Inhibition of Hepatocarcinogenesis by Interferon Therapy. *Ann Intern Med* 1999; 131: 174–81.
13. Toyoda H, Kumada T, Tokuda A, *et al.* Long-term follow-up of sustained responders to interferon therapy, in patients with chronic hepatitis C. *J Viral Hepat* 2000; 7: 414–9.
14. Enokimura N, Shiraki K, Kawakita T, *et al.* Hepatocellular carcinoma development in sustained viral responders to interferon therapy in patients with chronic hepatitis C. *Anticancer Res* 2003; 23: 593–6.
15. Makiyama A, Itoh Y, Kasahara A, *et al.* Characteristics of patients with chronic hepatitis C who develop hepatocellular carcinoma after a sustained response to interferon therapy. *Cancer* 2004; 101: 1616–22.
16. Tamori A, Nishiguchi S, Shiomi S, *et al.* Hepatitis B virus DNA integration in hepatocellular carcinoma after interferon-induced

disappearance of hepatitis C virus. *Am J Gastroenterol* 2005; 100: 1748–53.
17. Radkowski M, Gallegos-Orozco JF, Jablonska J, *et al.* Persistence of hepatitis C virus in patients successfully treated for chronic hepatitis C. *Hepatology* 2005; 41: 106–14.
18. Tamori A, Yamanishi Y, Kawashima S, *et al.* Alteration of gene expression in human hepatocellular carcinoma with integrated hepatitis B virus DNA. *Clin Cancer Res* 2005; 11: 5821–6.
19. Desmet VJ, Gerber M, Hoofnagle JH, *et al.* Classification of chronic hepatitis: diagnosis, grading and staging. *Hepatology* 1994; 19: 1513–20.
20. King MP, Attardi G. Human cells lacking mtDNA: repopulation with exogenous mitochondria by complementation. *Science* 1989; 246: 500–3.
21. Hayashi H, Sugio K, Matsumata T, *et al.* The clinical significance of p53 gene mutation in hepatocellular carcinomas from Japan. *Hepatology* 1995; 22: 1702–7.
22. Herman JG, Graff JR, Myohanen S, *et al.* Methylation-specific PCR: a novel PCR assay for methylation status of CpG islands. *Proc Natl Acad Sci USA* 1996; 93: 9821–96.
23. Zysman MA, Chapman WB, Bapat B. Considerations when analyzing the methylation status of PTEN tumor suppressor gene. *Am J Pathol* 2002; 160: 795–800.
24. To KF, Leung WK, Lee TL, *et al.* Promoter hypermethylation of tumor-related genes in gastric intestinal metaplasia of patients with and without gastric cancer. *Int J Cancer* 2002; 102: 623–8.
25. Tamori A, Nishiguchi S, Nishikawa M, *et al.* Correlation between clinical characteristics and mitochondrial D-loop DNA mutations in hepatocellular carcinoma. *J Gastroenterol* 2004; 39: 1063–8.
26. Nishikawa M, Nishiguchi S, Kioka K, *et al.* Interferon reduces somatic mutation of mitochondrial DNA in liver tissues from chronic viral hepatitis patients. *J Viral Hepat* 2005; 12: 494–8.
27. Huang LR, Hsu HC. Cloning and expression of CD24 gene in human hepatocellular carcinoma: a potential early tumor marker gene correlates with p53 mutation and tumor differentiation. *Cancer Res* 1995; 55: 4717–21.
28. Schagdarsurengin U, Wilkens L, Steinemann D, *et al.* Frequent epigenetic inactivation of the RASSF1A gene in hepatocellular carcinoma. *Oncogene* 2003; 22: 1866–71.
29. Matsuda Y, Ichida T, Matsuzawa J, *et al.* p16(INK4) is inactivated by extensive CpG methylation in human hepatocellular carcinoma. *Gastroenterology* 1999; 116: 394–400.
30. Liew CT, Li HM, Lo KW, *et al.* High frequency of p16INK4A gene alterations in hepatocellular carcinoma. *Oncogene* 1999; 18: 789–95.
31. Li X, Hui AM, Sun L, *et al.* p16INK4A hypermethylation is associated with hepatitis virus infection, age, and gender in hepatocellular carcinoma. *Clin Cancer Res* 2004; 10: 7484–9.
32. Fukai K, Yokosuka O, Imazeki F, *et al.* Methylation status of p14ARF, p15INK4b, and p16INK4a genes in human hepatocellular carcinoma. *Liver Int* 2005; 25: 1209–16.
33. Jin M, Piao Z, Kim NG, *et al.* p16 is a major inactivation target in hepatocellular carcinoma. *Cancer* 2000; 89: 60–8.
34. Wong IH, Lo YM, Yeo W, *et al.* Frequent p15 promoter methylation in tumor and peripheral blood from hepatocellular carcinoma patients. *Clin Cancer Res* 2000; 6: 3516–21.
35. Forman D, Webb P, Parsonnet J. *H. pylori* and gastric cancer. *Lancet* 1994; 343: 243–4.
36. Forman D, Newell DG, Fullerton F, *et al.* Association between infection with *Helicobacter pylori* and risk of gastric cancer: evidence from a prospective investigation. *BMJ* 1991; 302: 1302–5.
37. Maekita T, Nakazawa K, Mihara M, *et al.* High levels of aberrant DNA methylation in *Helicobacter pylori*-infected gastric mucosae and its possible association with gastric cancer risk. *Clin Cancer Res* 2006; 12: 989–95.
38. Tatematsu M, Tsukamoto T, Mizoshita T. Role of *Helicobacter pylori* in gastric carcinogenesis: the origin of gastric cancers and heterotopic proliferative glands in Mongolian gerbils. *Helicobacter* 2005; 10: 97–106.
39. Ushijima T, Nakajima T, Maekita T. DNA methylation as a marker for the past and future. *J Gastroenterol* 2006; 41: 401–7.
40. Alter MJ. Epidemiology of hepatitis C in the West. *Semin Liver Dis* 1995; 15: 5–14.

Comparative Immunology, Microbiology and Infectious Diseases xxx (2010) xxx–xxx

Contents lists available at ScienceDirect

Comparative Immunology, Microbiology and Infectious Diseases

journal homepage: www.elsevier.com/locate/cimid

Evaluation of a recombinant measles virus expressing hepatitis C virus envelope proteins by infection of human PBL-NOD/Scid/Jak3null mouse

Masaaki Satoh[a], Makoto Saito[a], Kohsuke Tanaka[a], Sumako Iwanaga[b], Salem Nagla Elwy Salem Ali[a,d], Takahiro Seki[e,1], Seiji Okada[b], Michinori Kohara[c], Shinji Harada[d], Chieko Kai[e], Kyoko Tsukiyama-Kohara[a,*]

[a] Department of Experimental Phylaxiology, Faculty of Life Sciences, Kumamoto University, 1-1-1 Honjo, Kumamoto-city, Kumamoto 860-8556, Japan
[b] Division of Hematopoiesis, Center for AIDS Research, Kumamoto University, Japan
[c] Department of Microbiology and Cell Biology, Tokyo Metropolitan Institute of Medical Science, Japan
[d] Department of Medical Virology, Faculty of Life Sciences, Kumamoto University, Japan
[e] Laboratory of Animal Research Center, Institute of Medical Science, University of Tokyo, Japan

ARTICLE INFO

Article history:
Received 27 January 2010
Accepted 21 February 2010

Keywords:
MV
HCV
E1
E2
Human PBL
NOD/Scid/Jak3null mouse

ABSTRACT

In this study, we infected NOD/Scid/Jak3null mice engrafted human peripheral blood leukocytes (hu-PBL-NOJ) with measles virus Edmonston B strain (MV-Edm) expressing hepatitis C virus (HCV) envelope proteins (rMV-E1E2) to evaluate the immunogenicity as a vaccine candidate. Although human leukocytes could be isolated from the spleen of mock-infected mice during the 2-weeks experiment, the proportion of engrafted human leukocytes in mice infected with MV (10^3–10^5 pfu) or rMV-E1E2 (10^4 pfu) was decreased. Viral infection of the splenocytes was confirmed by the development of cytopathic effects (CPEs) in co-cultures of splenocytes and B95a cells and verified using RT-PCR. Finally, human antibodies against MV were more frequently observed than E2-specific antibodies in serum from mice infected with a low dose of virus (MV, 10^0–10^1 pfu, and rMV-E1E2, 10^1–10^2 pfu). These results showed the possibility of hu-PBL-NOJ mice for the evaluation of the immunogenicity of viral proteins.

1. Introduction

Hepatitis C virus (HCV) is a member of the *Flaviviridae* family and is the causative agent of both chronic hepatitis and hepatocellular carcinoma (HCC) [1–3]. 170 million people are infected with HCV worldwide [4,5]. Despite prevention efforts and advanced treatment strategies, including combined PEGylated alpha interferron (PEGIFN-α) and ribavirin therapy [6,7], the clinical efficacy of this treatment is limited [8,9]. Alternative novel antiviral agents that have been shown to elicit effective responses in chronically infected patients, such as inhibitors of viral protease, helicase, and polymerase, are currently being developed but are expensive [10]. Therefore, the development of an effective vaccine that either induces the production of high-titer, long-lasting, and cross-reactive neutralising antibodies or induces a cellular immune response is important.

Immunological approaches to control HCV infection have proven to be ineffective, in part because HCV adapts to escape from the host immune system [11]. Furthermore, a high percentage of immunocompetent individuals

* Corresponding author. Tel.: +81 96 373 5560; fax: +81 96 373 55620.
E-mail address: kkohara@kumamoto-u.ac.jp (K. Tsukiyama-Kohara).
[1] Present address: Virology, Shionogi Research Laboratories, Shionogi & Co Ltd, Osaka, Japan.

0147-9571/$ – see front matter © 2010 Elsevier Ltd. All rights reserved.
doi:10.1016/j.cimid.2010.02.006

are infected by HCV despite their ability to mount an active immune response [12]. A preventive HCV vaccine is required to protect unexposed individuals from HCV infection. This vaccine will most likely need to target the viral envelope glycoprotein, E1 and E2, and must also be bivalent, safe, and provide long-lasting protective immunity. To address this challenge, we evaluated the immunogenicity of a live-attenuated recombinant vector derived from the pediatric measles virus (MV) that expresses HCV antigens. The MV vaccine is a well-known, live-attenuated vaccine and has proven to be one of the safest, most stable, and effective human vaccines [13]. This vaccine is produced on a large scale in many countries and used at low cost through the Extended Program on Immunisation of the WHO [14,15]. While this vaccine has been shown to induce life-long immunity with a single dose, boosting is effective. Efforts to develop vaccines using recombinant MV expressing different proteins derived from dengue virus [16,17], human immunodeficiency virus (HIV) [18–21], Human papilloma virus (HPV) [22], Severe acute respiratory syndrome (SARS) [23], or West Nile virus (WNV) [24] have been described. We constructed a recombinant MV expressing the E1 and E2 envelope glycoproteins of HCV (rMV-E1E2) [25] and demonstrated that this virus could infect B95a cells and express HCV E1.

HCV research has long been hampered by the lack of an animal model that reproduces HCV infection in humans. The model in which severe combined immunodeficient (SCID) mice are transplanted with human peripheral blood leukocyte (PBL) is a well-established system to study human immunity (hu-PBL-SCID). This mouse develops all human lymphoid cell lineages that repopulate the animal's lymphoid organs. Our group previously generated the non-obese diabetic (NOD)/SCID/Janus kinase 3 (Jak3) knockout (NOJ) mouse model and then established a human hemolymphoid system in this mouse [26,27]. In this study, we infect human PBL-transplanted NOJ mice with MV and rMV-E1E2 and then characterise the humoral immune responses elicited by the transplanted human cells, in order to evaluate rMV-E1E2 as a vaccine candidate.

2. Materials and methods

2.1. Cells

B95a cells, a marmoset B cell line [28], were used for viral titration and rescue, and were maintained in RPMI 1640 medium supplemented with 10% heat-inactivated foetal calf serum (FCS).

2.2. Plasmid construction and viral rescue

The cDNAs encoding HCV E1 and E2 were obtained from the plasmid HCR6CNS2 [29]. We used replication-competent MV-based vectors (pMV; Edmonston B strain of MV) [25]. The E1 and E2 cDNAs were cloned into the *Fse* I site of pMV and the resulting clone, pMV-E1E2, was used to rescue the infectious recombinant MV expressing the HCV envelope glycoproteins (rMV-E1E2), as reported previously [30].

2.3. Generation of humanised mice

Mice were reconstituted as described previously [26,27]. The NOD/SCID/JAK3^{null} strain was established by backcrossing JAK3^{null} and the NOD Cg-Prkdc^{Scid} strains for ten generations. All animal experiments were performed according to the guidelines of Institutional Animal Committee or Ethics Committee of Kumamoto University.

2.4. Preparation of human blood leukocytes and transplantation

Peripheral blood leukocytes were isolated from blood donors using Ficoll–Hypaque density gradient centrifugation. A total of 5×10^6 cells were transplanted into the spleen of irradiated (2 Gy) 4-week-old mice.

2.5. MV and MV-E1E2 infection

We injected 10^0–10^5 pfu of MV or 10^0–10^2 or 10^4 pfu of MV-E1E2 intraperitoneally for MV and MV-E1E2 infection, respectively. As a negative control, a group of mice was injected with RPMI 1640. Mice were monitored for 2 weeks and then euthanised. The spleens and peripheral blood were collected for analysis.

2.6. Flow cytometry

Isolated splenocytes were stained with APC-Cy7-conjugated anti-mouse CD45 (BD Pharmingen) to detect the murine leukocytes and either APC- or pacific blue-conjugated anti-human CD45 (DAKO) to detect human leukocytes. All data were analysed using FlowJo (Tree Star).

2.7. Confirmation of viral infection

The viral infection of the human leukocytes was confirmed using co-culture with B95a cells followed by RT-PCR. Suspensions of isolated splenocytes were co-cultured with B95a cells and the formation of cytopathic effects (CPEs) was monitored for 2 weeks. Additionally, RNA was isolated from the supernatant of the co-cultures using ISOGEN-LS (Nippon gene) according to manufacturer's instructions. MV RNA was detected using reverse transcript-PCR (RT-PCR) with the sense primer, 5′-ACTCGGTATCACTGCCGAGGATGCAAGGC-3′ (1256–1284) and anti-sense primer 5′-CAGCGTCGTCATCGCTCTCTCC-3′ (2077–2056) or 5′-atggcagaagagcaggcacg-3′ (1807–1826). HCV E1 or E2 was amplified using E1-S-1051 5′-ccgttgctgggtggcactta-3′ and E1-AS-1314 5′-atcatcatgtcccaagccat-3′ or E2-S-1600 5′-ctggcacatcaacaggactg-3′ and E2-AS-1960 5′-aaggagcagcacgtctgtct-3′.

2.8. ELISA

Anti-MV antibody titers were determined by using an ELISA assay. 96-well plates were coated with a 25 μg/ml solution of MV-infected B95a lysate or recombinant E2-expressing baculovirus-infected Sf9 lysate as antigen, respectively. The plates were consecutively incubated with

Please cite this article in press as: Satoh M, et al. Evaluation of a recombinant measles virus expressing hepatitis C virus envelope proteins by infection of human PBL-NOD/Scid/Jak3null mouse. Comp Immunol Microbiol Infect Dis (2010), doi:10.1016/j.cimid.2010.02.006

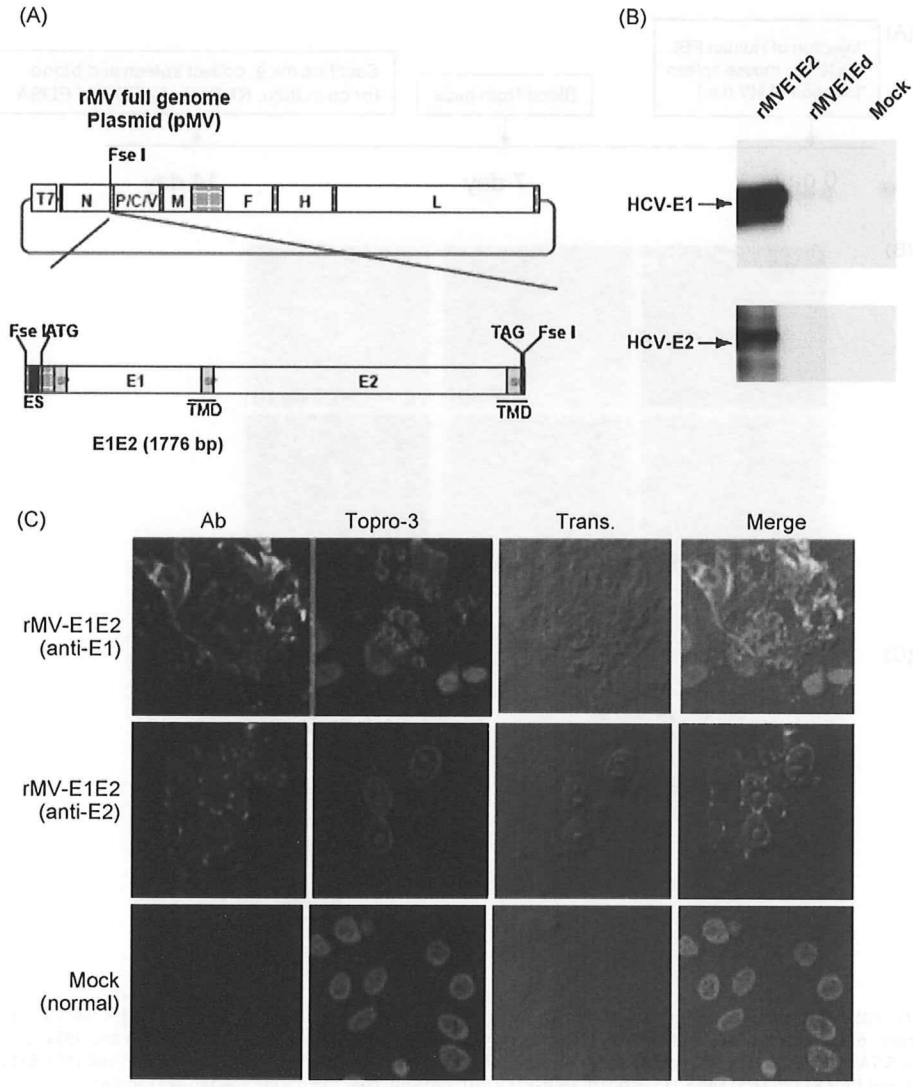

Fig. 1. Construction of the recombinant MV vectors. (A) The rMV full genome vector derived from the MV-Ed strain is illustrated in the upper panel and is labelled with letters as follows: N, nucleocapsid; P, phosphoprotein; M, matrix; F, fusion; H, hemagglutinin; and L, large. T7 indicates the T7 RNA polymerase promoter. The cDNA encoding the HCV envelope glycoproteins (E1 and E2) containing the signal peptide sequence (SP) and the transmembrane domain (TMD, underlined) regions, the N gene end signal (E), the P gene start signal (S), and the intercistronic region of the H protein genes at the 5′ end, which was flanked by Fse I sites at both ends, was introduced into the unique Fse I site in between the N and P genes in the pMV vector. The resulting plasmid was designated pMV-E1E2. (B) The HCV E1 and E2 proteins were detected in rMV-E1E2-, rMV-Ed- and mock-infected B95a cells by western blot with MoAb 384 and 544 (arrows). (C) rMV-E1E2-infected B95a cells were stained with MoAb 299 (anti-E1) or MoAb 187 (anti-E2) and analysed by immunofluorescence. Nuclei were stained with Topro-3 and the bright field and merged images are indicated (400×).

sera (1:100) recovered from hu-PBL-NOJ mice, peroxidase-conjugated rabbit-human IgG (DAKO), and TMB Peroxidase EIA Substrate Kit (Bio-Rad) at 37 °C for 1 h. Optimal density values were measured at 450 nm.

An anti-MV-NP antibody (Millipore, MA, USA) and normal mouse serum (NMS) were used as positive control and negative control respectively.

2.9. Western blot analysis

Total protein extracts from E2-expressing baculovirus-infected Sf9 lysate were separated by SDS-PAGE. The primary antibodies used for Western blots were as follows: sera from mice (1:100) and anti-E2 monoclonal antibody (1:5000). Peroxidase-conjugated secondary antibodies were added and incubated with the mixture for 1 h at room temperature.

3. Results

3.1. Construction of recombinant measles virus expressing E1 and E2

The HCV genes corresponding to the envelope proteins E1 and E2 were sub-cloned in between the N and P genes of the MV vector (Fig. 1A). The HCV E1 and E2 genes included

Please cite this article in press as: Satoh M, et al. Evaluation of a recombinant measles virus expressing hepatitis C virus envelope proteins by infection of human PBL-NOD/Scid/Jak3null mouse. Comp Immunol Microbiol Infect Dis (2010), doi:10.1016/j.cimid.2010.02.006

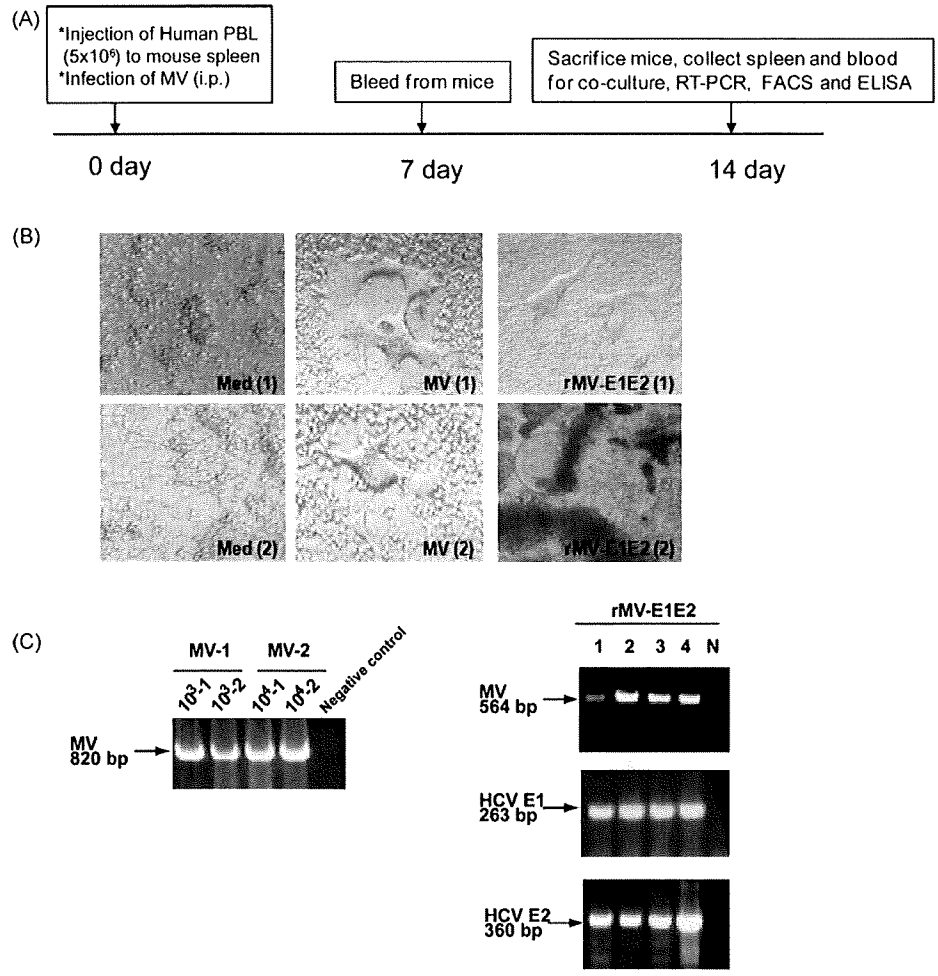

Fig. 2. Infection of hu-PBL-NOD/Scid mice with rMV and rMV-E1E2. (A) Course of infection of hu-PBL-NOD/SCID mice with MV and rMV-E1E2. (B) CPE formation in co-cultures of splenocytes isolated from MV- (MV1, 2), rMV-E1E2-, or mock-infected hu-PBL-NOD/SCID and B95a cells (40× magnification). (C) Detection of viral RNA by RT-PCR. Detection of MV in MV-1- or 2-infected mouse splenocyte co-cultures (820 bp) and rMV-E1E2-infected splenocyte co-cultures (564 bp), and HCV E1 (263 bp) and E2 (360 bp) in rMV-E1E2 (10^4 pfu)-infected splenocyte co-cultures (arrows).

the putative signal peptide sequences at the N terminus and the transmembrane domain at the C terminus [31]. The plasmid vector pMV-E1E2 was introduced with supporting plasmids into 293T cells to rescue the recombinant viruses. The expression of the E1 and E2 proteins by rMV-E1E2 was examined by Western blot (Fig. 1B) and immunofluorescence (Fig. 1C).

3.2. *Infection of hu-PBL-NOJ mice with MV and rMV-E1E2*

All hu-PBL-NOJ mouse infections were observed for 14 days (Fig. 2A). Infections with MV and rMV-E1E2 were confirmed by first co-culturing the human leukocytes isolated from the spleens of infected mice with B95a cells and then verifying the presence of virus by RT-PCR. In all the MV (10^3–10^4 pfu) or rMV-E1E2 (10^4 pfu)-infected hu-PBL-NOJ mice, CPEs were observed in co-cultures with splenocytes (Table 1; Fig. 2B). The results of the co-culture assays are in agreement with results that were obtained by RT-PCR; positive bands were observed in the mice infected with 10^3–10^4 pfu of MV and 10^4 pfu of rMV-E1E2 (Fig. 2C). These results demonstrate that the rescued MV and rMV-E1E2 are able to infect transplanted human PBL.

Table 1
Summary of MV and MV-E1E2 infection of hu-PBL-NOJ mice.

Virus	Amount of virus (PFU)	No. tested	CPE	RT-PCR
Mock	Medium	7	0/7	0/7
MV	10^0	3	0/3	0/3
	10^1	3	0/3	0/3
	10^2	3	0/3	0/3
	10^3	2	2/2	2/2
	10^4	2	2/2	2/2
MV-E1E2	10^0	3	0/3	0/3
	10^1	3	0/3	0/3
	10^2	3	0/3	1/3
	10^4	4	4/4	4/4

Please cite this article in press as: Satoh M, et al. Evaluation of a recombinant measles virus expressing hepatitis C virus envelope proteins by infection of human PBL-NOD/Scid/Jak3null mouse. Comp Immunol Microbiol Infect Dis (2010), doi:10.1016/j.cimid.2010.02.006

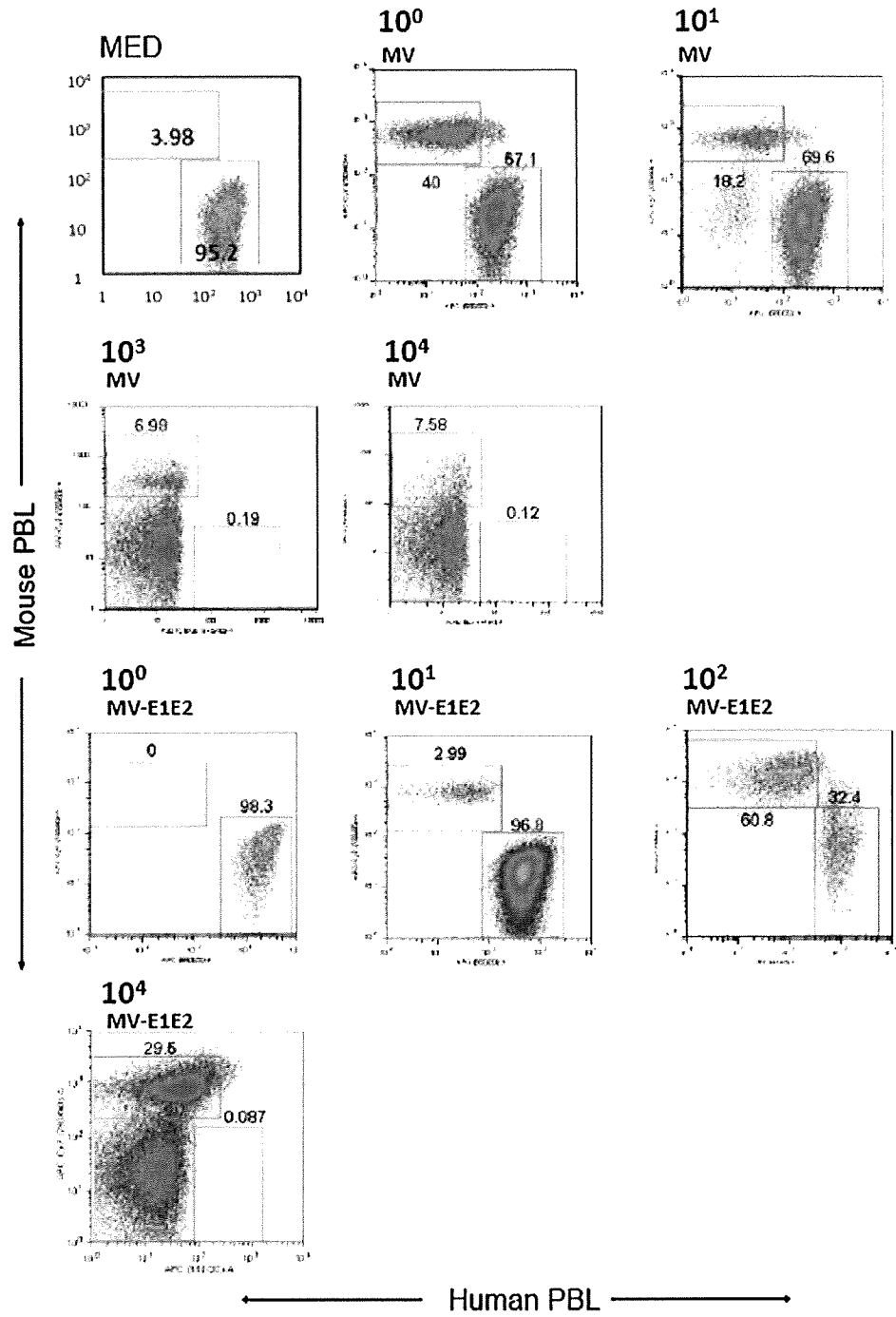

Fig. 3. Flow cytometric analysis of splenocytes isolated from hu-PBL-NOJ mice inoculated with medium, MV-Ed (10^0–10^4 pfu), or rMV-E1E2 (10^0–10^2 or 10^4 pfu). Splenocytes, consisting of both human and murine cells, were stained with antibodies against human or mouse CD45. Representative flow cytometric profiles of each group of infected mice are shown. The percentages of mouse and human leukocytes are shown.

3.3. Proportion of engrafted human leukocytes in MV- and rMV-E1E2- infected hu-PBL-NOJ mice

We also examined the splenocytes of infected mice simultaneously, using flow cytometry to determine the proportion of human cells in the spleen (Fig. 3, Table 2). In the MV-infected hu-PBL-NOJ mice, a population of human leukocytes was observed in the mice that were infected with 10^0–10^1 pfu, whereas few human leukocytes were observed in mice infected with 10^2–10^4 pfu. In contrast, in the rMV-E1E2-infected mice, a population of human leukocytes was detected in mice that were inoculated with 10^0–10^2 pfu. The ratio of human leukocytes settlement in both groups of mice was inversely correlated

Please cite this article in press as: Satoh M, et al. Evaluation of a recombinant measles virus expressing hepatitis C virus envelope proteins by infection of human PBL-NOD/Scid/Jak3null mouse. Comp Immunol Microbiol Infect Dis (2010), doi:10.1016/j.cimid.2010.02.006

Table 2
Proportion of human peripheral leukocytes in the spleen of MV-, rMV-E1E2, or mock-infected hu-PBL-NOJ mice.

Virus	Amount of virus (PFU)	No. tested	huPBL settlement (average ± S.D.%)
Mock	Medium	6	90.9 ± 13.1
MV	10^0	3	92.7 ± 11.2
	10^1	3	58.4 ± 50.6
	10^2	3	55.1 ± 49.9
	10^3	4	4.9 ± 6
	10^4	2	1.7
MV-E1E2	10^0	2	79.6
	10^1	2	96.0
	10^2	3	56.2 ± 36.2
	10^4	3	0.34 ± 0.4

with the results from the RT-PCR and co-culture assays (Table 1).

3.4. Humoral response of MV- and rMV-E1E2-infected hu-PBL-NOJ mice

To examine the immune response against MV and rMV-E1E2 by the transplanted human PBLs, we measured human MV- or HCV-specific antibodies using an ELISA with an MV-infected B95a cell lysate (Fig. 4A) or recombinant HCV E2 protein (Fig. 4B). A significant amount of human antibody against MV antigens was detected in the sera from mice that were infected with MV (10^0–10^1 pfu) or rMV-E1E2 (10^1–10^2 pfu) (Fig. 4A and B). However, only one mouse, which was infected with 10^2 pfu of rMV-E1E2, generated human antibodies against HCV E2 (Fig. 5A). The antibody responses in this mouse were confirmed by Western blot analysis (Fig. 5B).

4. Discussion

The development of a vaccine against HCV has relied on several tools, including recombinant proteins and peptides that are derived from HCV antigens [12,32–34]. HCV E1 E2 proteins play essential roles in the entry of HCV into host cells. Therefore, these proteins represent ideal targets for neutralising antibodies to block viral entry.

Several studies have used the measles virus as a vector for expression of other viral proteins [16,17]. In this study, we examined the infectivity of a rescued Edmonston B strain of MV and a recombinant rMV-E1E2 that was constructed using reverse genetics [25,30]. We demonstrate that these viruses can infect hu-PBL-NOJ mice. This is the first report demonstrating that rescued virus, including a recombinant virus, can infect hu-PBL-NOJ mice. Furthermore, an adequate viral titer could control the generation of antibodies in these mice. Based on the flow cytometry data, most of the human leukocytes disappeared following infection with high virus titer (10^3–10^4 pfu) and human antibody was not detected in these mice (data not shown). In contrast, a population of human leukocytes was detected in the mice that were inoculated with a lower dose of virus (10^0–10^2 pfu). In addition, we could detect human antibodies in the serum of mice that were infected with a low dose of virus, suggesting that this viral titer range is suitable for the induction of an antibody response that targets rMVs in the hu-PBL-NOJ mouse system. This range of virus concentration is adequate for antibody production and the resulting antibody response might suppress the viral growth of 10^0–10^1 pfu MVs in hu-PBL-NOJ mice.

The humanised mouse is a promising model for studying the transmission of the live, attenuated Edmonston B strain of the measles virus. There have been several reports detailing the infection of experimental transgenic mice that

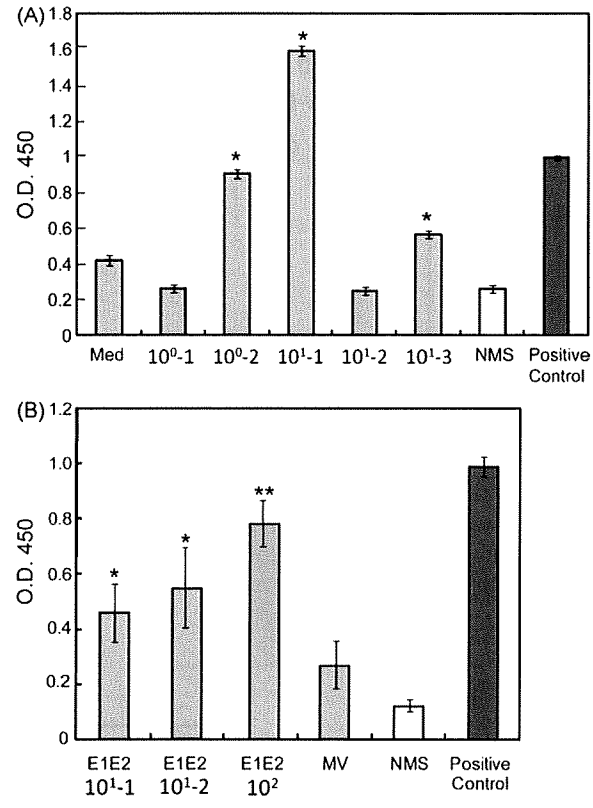

Fig. 4. Detection of human MV-specific antibodies in the serum of rMV- or rMV-E1E2-infected mice. (A) Serum (1:100) from MV-infected mice (10^0–10^1 pfu) was analysed by ELISA using an MV-infected B95a cell lysate as the target. An anti-MV-NP antibody was used as a positive control and NMS indicates normal mouse serum. The asterisk (*) indicates a significant reaction ($p < 0.01$) compared to the medium alone control. (B) Serum (1:100) from rMV-E1E2-infected mice (10^1–10^2 pfu) was analysed by ELISA. An anti-MV-NP antibody was used as a positive control and NMS indicates normal mouse serum. The double asterisk (**) indicates a highly significant reaction ($p < 0.001$) compared to NMS and a single asterisk (*) indicates a significant reaction ($p < 0.05$) compared to NMS.

Please cite this article in press as: Satoh M, et al. Evaluation of a recombinant measles virus expressing hepatitis C virus envelope proteins by infection of human PBL-NOD/Scid/Jak3null mouse. Comp Immunol Microbiol Infect Dis (2010), doi:10.1016/j.cimid.2010.02.006

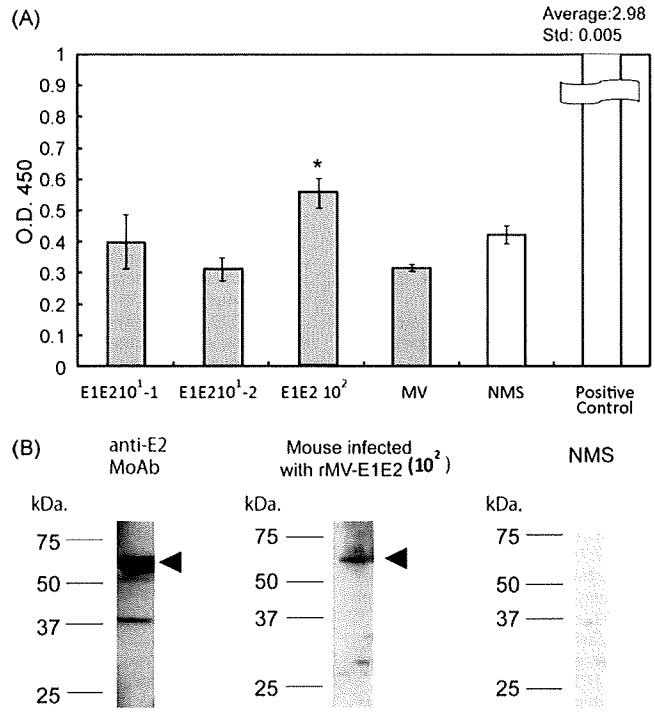

Fig. 5. Detection of E2-specific antibodies using ELISA and western blot. (A) Baculovirus-expressed E2 protein was used as the ELISA antigen and serum (diluted 1:100) from rMV-E1E2-infected mice (10^1–10^2 pfu) was analysed. Anti-E2 monoclonal antibody (MoAb 544) was used as positive control. The asterisk (*) indicates a significant reaction ($p < 0.05$) compared to NMS. (B) An anti-E2 monoclonal antibody (MoAb 544), serum from rMV-E1E2 infected mice (1:100), or normal mouse serum (1:100) was used as primary antibodies in a western blot to detect baculovirus-expressed E2 protein. The triangles indicate bands that correspond to HCV E2.

expresses human CD46 and CD150 with some strains of measles virus [35,36]. However, unlike in other animal models, a population of human cells is the target of the virus in this study. Furthermore, the use of hu-PBL-NOJ mice allows one to monitor the immune response that is generated by human leukocytes against the immunogen. Based on our results, hu-PBL-NOJ mice should be a useful tool for studying the immune response during early MV or rMV-E1E2 infection. Since there is no animal model of HCV infection, monitoring the immune response of human leukocytes permits the accurate evaluation of potential vaccine candidates.

We detected a significant amount of MV-specific antibodies in the rMV-E1E2-infected mice ($n = 3$). However, only one mouse produced E2-specific antibodies and no mice produced E1-specific antibodies. This result could be explained by the hypothesis that the immunogenicity of the E1 and E2, especially E1 protein might be lower than the immunogenicity of the MV proteins, an observation that is consistent with previous studies [37–40].

Further development of the hu-PBL-NOJ mouse model system will allow us to characterise not only the immediate immune response, but also the long-term evolution of the human immune response against measles virus and recombinant measles viruses. This system will make it possible to evaluate the immunogenicity of potential vaccine targets using human PBLs, which is indispensable for the development of an effective vaccine of HCV.

Acknowledgements

We would like to thank Drs. M.A. Billeter and K. Takeuchi for providing the MV Edmonston B strain rescue system, F. Ikeda and M. Yoneda for their technical support. This work was supported by grants from the Ministry of Health and Welfare of Japan, the Ministry of Education, Culture, Sports, Science and Technology of Japan, the Program for Promotion of Fundamental Studies in Health Sciences of the National Institute of Biomedical Innovation, and the Cooperative Research Project on Clinical and Epidemiological Studies of Emerging and Re-emerging Infectious Diseases.

References

[1] Di Bisceglie AM, Carithers Jr RL, Gores GJ. Hepatocellular carcinoma. Hepatology 1998;28(4):1161–5.
[2] Hayashi J, et al. Hepatitis C virus and hepatocarcinogenesis. Intervirology 1999;42(2–3):205–10.
[3] Michielsen PP, Francque SM, van Dongen JL. Viral hepatitis and hepatocellular carcinoma. World J Surg Oncol 2005;3:27.
[4] Global surveillance and control of hepatitis C. Report of a WHO Consultation organized in collaboration with the Viral Hepatitis Prevention Board, Antwerp, Belgium. J Viral Hepat, 1999;6(1):35–47.
[5] Zoulim F, et al. Clinical consequences of hepatitis C virus infection. Rev Med Virol 2003;13(1):57–68.
[6] Bruchfeld A, et al. Ribavirin treatment in dialysis patients with chronic hepatitis C virus infection—a pilot study. J Viral Hepat 2001;8(4):287–92.
[7] Mazzella G, et al. Alpha interferon treatment may prevent hepatocellular carcinoma in HCV-related liver cirrhosis. J Hepatol 1996;24(2):141–7.

Please cite this article in press as: Satoh M, et al. Evaluation of a recombinant measles virus expressing hepatitis C virus envelope proteins by infection of human PBL-NOD/Scid/Jak3null mouse. Comp Immunol Microbiol Infect Dis (2010), doi:10.1016/j.cimid.2010.02.006

[8] Kohara M, et al. Hepatitis C virus genotypes 1 and 2 respond to interferon-alpha with different virologic kinetics. J Infect Dis 1995;172(4):934–8.
[9] Nakamura H, et al. Interferon treatment for patients with chronic hepatitis C infected with high viral load of genotype 2 virus. Hepatogastroenterology 2002;49(47):1373–6.
[10] Bukh J, et al. Studies of hepatitis C virus in chimpanzees and their importance for vaccine development. Intervirology 2001;44(2–3):132–42.
[11] Bowen DG, Walker CM. Mutational escape from CD8+ T cell immunity: HCV evolution, from chimpanzees to man. J Exp Med 2005;201(11):1709–14.
[12] Lechmann M, Liang TJ. Vaccine development for hepatitis C. Semin Liver Dis 2000;20(2):211–26.
[13] Combredet C, et al. A molecularly cloned Schwarz strain of measles virus vaccine induces strong immune responses in macaques and transgenic mice. J Virol 2003;77(21):11546–54.
[14] Naniche D, et al. Decrease in measles virus-specific CD4 T cell memory in vaccinated subjects. J Infect Dis 2004;190(8): 1387–95.
[15] Ovsyannikova IG, et al. Frequency of measles virus-specific CD4+ and CD8+ T cells in subjects seronegative or highly seropositive for measles vaccine. Clin Diagn Lab Immunol 2003;10(3):411–6.
[16] Brandler S, et al. Pediatric measles vaccine expressing a dengue antigen induces durable serotype-specific neutralizing antibodies to dengue virus. PLoS Negl Trop Dis 2007;1(3):e96.
[17] Brandler S, Tangy F. Recombinant vector derived from live attenuated measles virus: potential for flavivirus vaccines. Comp Immunol Microbiol Infect Dis 2008;31(2–3):271–91.
[18] Guerbois M, et al. Live attenuated measles vaccine expressing HIV-1 Gag virus like particles covered with gp160DeltaV1V2 is strongly immunogenic. Virology 2009;388(1):191–203.
[19] Liniger M, et al. Recombinant measles viruses expressing single or multiple antigens of human immunodeficiency virus (HIV-1) induce cellular and humoral immune responses. Vaccine 2009;27(25–26):3299–305.
[20] Lorin C, et al. A recombinant live attenuated measles vaccine vector primes effective HLA-A0201-restricted cytotoxic T lymphocytes and broadly neutralizing antibodies against HIV-1 conserved epitopes. Vaccine 2005;23(36):4463–72.
[21] Lorin C, et al. A single injection of recombinant measles virus vaccines expressing human immunodeficiency virus (HIV) type 1 clade B envelope glycoproteins induces neutralizing antibodies and cellular immune responses to HIV. J Virol 2004;78(1):146–57.
[22] Cantarella G, et al. Recombinant measles virus-HPV vaccine candidates for prevention of cervical carcinoma. Vaccine 2009; 27(25–26):3385–90.
[23] Liniger M, et al. Induction of neutralising antibodies and cellular immune responses against SARS coronavirus by recombinant measles viruses. Vaccine 2008;26(17):2164–74.
[24] Despres P, et al. Live measles vaccine expressing the secreted form of the West Nile virus envelope glycoprotein protects against West Nile virus encephalitis. J Infect Dis 2005;191(2):207–14.
[25] Radecke F, et al. Rescue of measles viruses from cloned DNA. EMBO J 1995;14(23):5773–84.
[26] Okada S, et al. Early development of human hematopoietic and acquired immune systems in new born NOD/Scid/Jak3null mice intrahepatic engrafted with cord blood-derived CD34+ cells. Int J Hematol 2008;88(5):476–82.
[27] Hattori S, et al. Potent activity of a nucleoside reverse transcriptase inhibitor, 4'-ethynyl-2-fluoro-2'-deoxyadenosine, against human immunodeficiency virus type 1 infection in a model using human peripheral blood mononuclear cell-transplanted NOD/SCID Janus kinase 3 knockout mice. Antimicrob Agents Chemother 2009;53(9):3887–93.
[28] Kobune F, Sakata H, Sugiura A. Marmoset lymphoblastoid cells as a sensitive host for isolation of measles virus. J Virol 1990;64(2):700–5.
[29] Tsukiyama-Kohara K, et al. Activation of the CKI-CDK-Rb-E2F pathway in full genome hepatitis C virus-expressing cells. J Biol Chem 2004;279(15):14531–41.
[30] Yoneda M, et al. Rinderpest virus phosphoprotein gene is a major determinant of species-specific pathogenicity. J Virol 2004;78(12):6676–81.
[31] Op De Beeck A, Cocquerel L, Dubuisson J. Biogenesis of hepatitis C virus envelope glycoproteins. J Gen Virol 2001;82(Pt 11):2589–95.
[32] Beyene A, et al. Hepatitis C virus envelope glycoproteins and potential for vaccine development. Vox Sang 2002;83(Suppl 1):27–32.
[33] Seong YR, et al. Immunogenicity of the E1E2 proteins of hepatitis C virus expressed by recombinant adenoviruses. Vaccine 2001;19(20–22):2955–64.
[34] Stamataki Z, et al. Hepatitis C virus envelope glycoprotein immunization of rodents elicits cross-reactive neutralizing antibodies. Vaccine 2007;25(45):7773–84.
[35] Ohno S, et al. Measles virus infection of SLAM (CD150) knockin mice reproduces tropism and immunosuppression in human infection. J Virol 2007;81(4):1650–9.
[36] Sellin CI, et al. High pathogenicity of wild-type measles virus infection in CD150 (SLAM) transgenic mice. J Virol 2006;80(13):6420–9.
[37] Falkowska E, et al. Hepatitis C virus envelope glycoprotein E2 glycans modulate entry, CD81 binding, and neutralization. J Virol 2007;81(15):8072–9.
[38] Helle F, et al. The neutralizing activity of anti-hepatitis C virus antibodies is modulated by specific glycans on the E2 envelope protein. J Virol 2007;81(15):8101–11.
[39] Jackson P, et al. Reactivity of synthetic peptides representing selected sections of hepatitis C virus core and envelope proteins with a panel of hepatitis C virus-seropositive human plasma. J Med Virol 1997;51(1):67–79.
[40] Hoofnagle JH. Course and outcome of hepatitis C. Hepatology 2002;36(5 Suppl 1):S21–9.

Please cite this article in press as: Satoh M, et al. Evaluation of a recombinant measles virus expressing hepatitis C virus envelope proteins by infection of human PBL-NOD/Scid/Jak3null mouse. Comp Immunol Microbiol Infect Dis (2010), doi:10.1016/j.cimid.2010.02.006

JOURNAL OF VIROLOGY, Jan. 2010, p. 303–311 Vol. 84, No. 1
0022-538X/10/$12.00 doi:10.1128/JVI.01448-09

Pathogenesis of Hepatitis C Virus Infection in *Tupaia belangeri*▽†

Yutaka Amako,[1] Kyoko Tsukiyama-Kohara,[1,2] Asao Katsume,[1,3] Yuichi Hirata,[1] Satoshi Sekiguchi,[1] Yoshimi Tobita,[1] Yukiko Hayashi,[4] Tsunekazu Hishima,[4] Nobuaki Funata,[4] Hiromichi Yonekawa,[5] and Michinori Kohara[1]*

Department of Microbiology and Cell Biology, Tokyo Metropolitan Institute of Medical Science, 2-1-6, Kamikitazawa, Setagaya-ku, Tokyo 156-0057, Japan[1]; Department of Experimental Phylaxiology, Faculty of Medical and Pharmaceutical Sciences, Kumamoto University, 1-1-1 Honjo Kumamoto City, Kumamoto 860-8556, Japan[2]; Fuji Gotemba Research Laboratory, Chugai Pharmaceutical Company, Ltd., 135, Komakado 1 Chome, Gotemba-shi, Shizuoka 412-8513, Japan[3]; Department of Pathology, Tokyo Metropolitan Komagome Hospital, 3-18-22 Honkomagome, Bunkyo-ku, Tokyo 113-8677, Japan[4]; and Laboratory of Animal Science, Tokyo Metropolitan Institute of Medical Science, 2-1-6, Kamikitazawa, Setagaya-ku, Tokyo 156-0057, Japan[5]

Received 14 July 2009/Accepted 5 October 2009

The lack of a small-animal model has hampered the analysis of hepatitis C virus (HCV) pathogenesis. The tupaia (*Tupaia belangeri*), a tree shrew, has shown susceptibility to HCV infection and has been considered a possible candidate for a small experimental model of HCV infection. However, a longitudinal analysis of HCV-infected tupaias has yet to be described. Here, we provide an analysis of HCV pathogenesis during the course of infection in tupaias over a 3-year period. The animals were inoculated with hepatitis C patient serum HCR6 or viral particles reconstituted from full-length cDNA. In either case, inoculation caused mild hepatitis and intermittent viremia during the acute phase of infection. Histological analysis of infected livers revealed that HCV caused chronic hepatitis that worsened in a time-dependent manner. Liver steatosis, cirrhotic nodules, and accompanying tumorigenesis were also detected. To examine whether infectious virus particles were produced in tupaia livers, naive animals were inoculated with sera from HCV-infected tupaias, which had been confirmed positive for HCV RNA. As a result, the recipient animals also displayed mild hepatitis and intermittent viremia. Quasispecies were also observed in the NS5A region, signaling phylogenic lineage from the original inoculating sequence. Taken together, these data suggest that the tupaia is a practical animal model for experimental studies of HCV infection.

Hepatitis C virus (HCV) is a small enveloped virus that causes chronic hepatitis worldwide (32). HCV belongs to the genus *Hepacivirus* of the family *Flaviviridae*. Its genome comprises 9.6 kb of single-stranded RNA of positive polarity flanked by highly conserved untranslated regions at both the 5′ and 3′ ends (4, 27, 29). The 5′ untranslated region harbors an internal ribosomal entry site (29) that initiates translation of a single open reading frame encoding a large polyprotein comprising about 3,010 amino acids (35). The encoded polyprotein is co- and posttranslationally processed into 10 individual viral proteins (15).

In most cases of human infection, HCV is highly potent and establishes lifelong persistent infection, which progressively leads to chronic hepatitis, liver steatosis, cirrhosis, and hepatocellular carcinoma (9, 16, 21). The most effective therapy for treatment of HCV infection is administration of pegylated interferon combined with ribavirin. However, the combination therapy is an arduous regimen for patients; furthermore, HCV genotype 1b does not respond efficiently (19). The prevailing scientific opinion is that a more viable option than interferon treatment is needed.

The chimpanzee is the only validated animal model for in vivo studies of HCV infection, and it is capable of reproducing most aspects of human infection (5, 18, 23, 28, 35, 36). The chimpanzee is also the only validated animal for testing the authenticity and infectivity of cloned viral sequences (8, 14, 35, 36). However, chimpanzees are relatively rare and expensive experimental subjects. Cross-species transmission from infected chimpanzees to other nonhuman primates has been tested but has proven unsuccessful for all species evaluated (1).

The tupaia (*Tupaia belangeri*), a tree shrew, is a small nonprimate mammal indigenous to certain areas of Southeast Asia (6). It is susceptible to infection with a wide range of human-pathogenic viruses, including hepatitis B viruses (13, 20, 31), and appears to be permissive for HCV infection (33, 34). In an initial report, approximately one-third of inoculated animals exhibited acute, transient infection, although none developed the high-titer sustained viremia characteristic of infection in humans and chimpanzees (33). The short duration of follow-up precluded any observation of liver pathology. In addition to the putative in vivo model, cultured primary hepatocytes from tupaias can be infected with HCV, leading to de novo synthesis of HCV RNA (37). These reports strongly support tupaias as a valid model for experimental studies of HCV infection. However, longitudinal analyses evaluating the clinical development and pathology of HCV-infected tupaias have yet to be exam-

* Corresponding author. Mailing address: Department of Microbiology and Cell Biology, The Tokyo Metropolitan Institute of Medical Science, 2-1-6, Kamikitazawa, Setagaya-ku, Tokyo 156-0057, Japan. Phone: 81-3-5316-3232. Fax: 81-3-5316-3137. E-mail: kohara-mc@igakuken.or.jp.

† Supplemental material for this article may be found at http://jvi.asm.org/.

▽ Published ahead of print on 21 October 2009.